AD NUMBER
AD360988
CLASSIFICATION CHANGES
TO: unclassified
FROM: confidential
LIMITATION CHANGES
TO: Approved for public release, distribution unlimited
FROM: Distribution authorized to U.S. Gov't. agencies only; Administrative/Operational Use; MAY 1965. Other requests shall be referred to Office of Naval Research, Arlington, VA 22203.
AUTHORITY
31 May 1977, DoDD 5200.10; ONR ltr, 14 Jun 1977

Doc. 5533.

CONFIDENTIAL

360988

FEASIBILITY OF DESIGN OF OMEGA ANTENNAS BY FERRITE-LOADING TECHNIQUES

Technical Report

Contract NOnr 3538(00)

Department of the Navy
Office of Naval Research
Washington, 25, D.C.

Reproduction in Whole or in Part is Permitted
for Any Purpose of the United States Government

DOWNGRADED AT 3 YEAR INTERVALS;
DECLASSIFIED AFTER 12 YEARS.
DOD DIR 5200.10

ITT FEDERAL LABORATORIES
a division of International Telephone and Telegraph Corporation
500 Washington Avenue Nutley, New Jersey 07110

MAY 1965

CONFIDENTIAL

TECHNICAL REPORT

FEASIBILITY OF DESIGN OF OMEGA ANTENNAS

BY FERRITE-LOADING TECHNIQUES

Contract NOnr 3358(00)
Office of Naval Research
Navy Department
Washington 25, D.C.

Prepared by: L. M. Vallese
A. M. Passalaqua
G. Rakowsky

Reviewed by: L. M. Vallese - Project Manager

Approved by: F. A. Muller - Director
Physical Sciences Laboratory

ITT FEDERAL LABORATORIES
A division of International Telephone and Telegraph Corporation
500 Washington Avenue Nutley, New Jersey 07110

TABLE OF CONTENTS

		PAGE
1.	INTRODUCTION	1
2.	THEORY OF FERRITE-LOADED RADIATORS	2
3.	INITIAL PROPOSAL OF FERRITE-LOADED OMEGA ANTENNA DESIGN	17
4.	REVIEW OF EXISTING VLF ANTENNA SYSTEMS	21
5.	RADIATION RESISTANCE OF VLF ANTENNAS	28
6.	DESIGN OF THE GROUND PLANE	29
7.	DESIGN OF THE TOP LOAD	36
8.	EXPERIMENTAL VERIFICATION OF LOW-FREQUENCY FERRITE ANTENNA DESIGN	38
9.	CONCLUSIVE REMARKS	41

CONFIDENTIAL

LIST OF FIGURES

FIGURE		PAGE
1	Cylindrical Coordinate System	14
2	Plots of Equations 29 and 30	15
3	Wavelength Reduction for Infinite Ferrite-Loaded Line	16
4	Preliminary Proposal of Omega Ferrite Antenna	
5	Alternate Preliminary Proposal of Omega Ferrite Antenna	
6	Jim Creek VLF Transmitting Antenna	
7	Diagram of the Annapolis, Md., Antenna	
8	Rocky Point Antenna	
9	Rugby GBR Transmitting Antenna	
10	Rugby GBR Transmitting Antenna Ground System	
11	Diagram of the Marion, Mass., and New Brunswick, N.J., VLF Transmitting Antennas	
12	Diagram of the VLF Antenna at Tuckerton, N.J.	
13	Examples of Top-Loaded Antennas	
14	Theoretical and Experimental Values of Radiation Resistance versus H/λ	
15	Experimental Values of R_r for Various Ferrite-Loaded Antennas versus $\bar{H}/\lambda$	
16	Phase and Density of Radial Ground Current	
17	Sketch of Antenna System	
18	Optimum and Terminal Spacing of Buried Conductors	
19	ΔR and ΔX vs r_t/λ ($h/\lambda = 0.25$)	
20	ΔR and ΔX vs r_t/λ ($h/\lambda = 0.1$ and 0.01)	
21	ΔR and ΔX vs r_t/λ (Parameter a/λ)	
22	ΔR and ΔX vs a/λ (Parameter r_t/λ)	
23	ΔR vs α/π	
24	ΔR vs h/λ ($\alpha = \pi/2$ or 0)	
25	ΔR and ΔX vs r_t/λ for Various Surface Impedance Values	
26	Relationship between S and Ground Conductivity	
27	Assumed Antenna Current Distribution	
28	Radial Density Component J_ρ^v vs ρ/h	
29	Surface Current Density J_s^h vs ρ/h at Two Azimuths ($h/\lambda = 0$)	
30	Surface Current Density J_s^h vs ρ/h at Two Azimuths ($h/\lambda = 0.06$)	

CONFIDENTIAL

31 L- and T-Type Loading
32 Ratio J_ϕ^h/J_φ^v for L-Type Loading
33 Ratio J_ϕ^h/J_φ^v for T-Type Loading ($h/\lambda = 0$)
34 Wavelength Shortening Ratio of 3" Ferrite Radiator vs Length
35 Input Resistance and Reactance of 100-Ft Ferrite Radiator
36 Radiation Pattern of 100' Ferrite Antenna

LIST OF TABLES

TABLE		PAGE
I	SUMMARY OF PROPERTIES OF FERRITE TOROIDS USED	12
II	RESONANT FERRITE MONOPOLES	13
III	SUMMARY OF VLF ANTENNA CHARACTERISTICS	27

1

FEASIBILITY OF DESIGN OF OMEGA ANTENNAS
BY FERRITE-LOADING TECHNIQUES

1. INTRODUCTION

The following Technical Report represents a summary of a theoretical and experimental investigation conducted under Contract NOnr 3358, NR 373-804 during the period January 1964 to May 1965, in order to verify and extend the calculations developed previously, under the same contract, for the design of an Omega Transmitting system, using ferrite-loading techniques. The data presented in the following report include some results obtained in the investigation of a ferrite-loaded Low Frequency transportable-type antenna.

Ferrite-loading techniques for transmitting antennas have been investigated extensively at ITT FEDERAL LABORATORIES under Contract NOnr 3358 for application to the design of VLF, LF, and HF radiators. In a previous Technical Report entitled "VLF Ferrite Antennas", dated November 1963, the theoretical analysis of linear loading was developed; in particular, the axial wavelength shortening ratio λ_z/λ_o, the height-to-air-wavelength ratio H/λ_o, the relative bandwidth, the radiation resistance and the radiation efficiency, the proximity interaction between unloaded and loaded conductors, etc., were studied. Experimental verifications conducted at H.F. (2 to 26 mc/s) provided excellent agreement with the theoretical calculations.

On the basis of these results, a design of transmitting antenna system for Omega application was developed. This consisted of a cage-type structure built with 500' ferrite-loaded monopoles, supported by means of 500' or 650' towers. The details of this design are summarized in a following Section. Extrapolating results obtained at HF, the principal characteristics of the antenna system, such as resonance wavelength for

given ferrite loading, radiation resistance, maximum radiated power, etc., were derived.

In order to provide a check of the validity of the extrapolation, an experimental investigation of a low-frequency antenna representing approximately a 10-to-1 model of the proposed Omega system was undertaken. The Federal Communications Commission granted ITT FEDERAL LABORATORIES an experimental Radio Station License for operation at 81.7 Kc/s and 69 Kc/s , with a maximum radiated power of 5000 watts. After a thorough study of ground-plane techniques and requirements, a site was selected at Nutley, N.J., and a 100'-high vertical monopole using ferrite-loading techniques was built. Permission for the erection of the required 100' towers was granted by the Federal Aviation Agency. Although, at the date of the writing of the present report, the investigation of the properties of this transmitting system has not yet been completed, a wealth of experimental results of great technical significance has been already obtained. These are presented in the following, along with conclusions and recommendations for application to the final Omega system design.

2. THEORY OF FERRITE-LOADED RADIATORS

The theory of linear ferrite-loaded antennas may be developed from consideration of an infinite cylindrical wire of diameter 2a coated with a uniform sheath of ferrite of diameter 2b (Fig. 1).

Consider an infinite straight conductor of infinite conductivity and radius a , surrounded by an uniform ferrite cylinder of inner radius a , and outer radius b , having permeability μ , and permittivity ϵ_1 . Using a cylindrical coordinate system ρ , θ , z , one finds that the electromagnetic field distribution may be expressed in terms of two Hertz vector potentials π_1 and π_2 both parallel to the z axis and such that their magnitudes satisfy the scalar wave equation:

$$\nabla^2 - \mu\epsilon \frac{\delta^2}{\delta t^2} - \mu \frac{\delta}{\delta t} \quad \psi = 0 \qquad (1)$$

Assuming harmonic time and space dependence, one may let, in general:

$$\psi = f (\rho , \theta) \exp (j\omega t - \beta z) \qquad (2)$$

where $f(\rho\theta)$ is a solution of the equation

$$\frac{1}{\rho}\frac{\delta}{\delta\rho}\left(\rho\frac{\delta f}{\delta\rho}\right)+\frac{1}{\rho^2}\frac{\delta^2 f}{\delta\theta^2}+(K^2-\beta^2)f=0 \qquad (3)$$

In the above equation, the coefficient K is expressed in terms of the characteristics of the medium; i.e.,

$$K^2=\omega^2-j\omega\mu\sigma \qquad (4)$$

and the coefficient β is the axial propagation constant; i.e.,

$$\beta = 2\pi/\lambda_z \qquad (5)$$

where λ_z is the wavelength along the z axis. The general expression of the electromagnetic field is derived from the vector potentials π_1 and π_2, using the following relations:

$$\overline{E} = \nabla\times\nabla\times\overline{\pi_1}+j\omega\mu\nabla\times\overline{\pi_2} \qquad (6)$$

$$\overline{H} = (\sigma+j\omega\epsilon)\overline{\pi_1}+\nabla\times\nabla\times\overline{\pi_2}$$

It is seen that the field derived from $\overline{\pi_1}$ has no axial magnetic field component, while the field derived from $\overline{\pi_2}$ has no axial electric field component; for this reason, the two field configurations are called respectively "transverse magnetic" and "transverse electric".

Clearly, the problem of interest in the present investigation falls into the class of transverse magnetic modes. We can proceed accordingly, neglecting $\overline{\pi_2}$ and solving Eq. 3 separately in region 1, (i.e., $a \leq \rho \leq b$), and in region 2 (i.e., $b \leq \rho \leq \infty$).

In region 1, we may let, in general,

$$E_{1z} = \sum_{n=0}^{\infty} \left[(A_{1n} J_n (h_{1n} \rho) + B_{1n} N_n (h_{1n} \rho) \right] \epsilon^{j(n\theta + \omega t - \beta_n z)} \tag{7}$$

$$H_{1z} = 0$$

and in region 2, we may let

$$E_{2z} = \sum_{n=0}^{\infty} C_{2n} \; H_n^{(1)} (h_{2n} \rho) \; \epsilon^{j(n\theta + \omega t - \beta_n z)} \tag{8}$$

In the above equations,

$$h_{1\,n}^{\;2} = K_1^{\,2} - \beta_n^{\,2}$$

$$h_{2\,n}^{\;2} = K_2^{\,2} - \beta_n^{\,2} \tag{9}$$

Since we are interested in fields which are distributed uniformly with respect to the angle θ, we shall limit our investigation to the zero-order mode only; i.e., $n = 0$. Hence, applying Equa. 7, we find:

Region 1

$$E_{1z} = \left[A_1 J_o (h_1 \rho) + B_1 N_o (h_1 \rho) \right] \epsilon^{j(\omega t - \beta z)} \tag{10}$$

$$E_{1\rho} = \frac{-j\beta}{\sqrt{K_1^{\,2} - \beta^2}} \left[A_1 J_1 (h_1 \rho) + B_1 N_1 (h_1 \rho) \right] \epsilon^{j(\omega t - \beta z)}$$

$$H_{1\theta} = \frac{-jK_1^{\,2}}{\omega \mu_1 \sqrt{K_1^{\,2} - \beta^2}} \left[A_1 J_1 (h_1 \rho) + B_1 N_1 (h_1 \rho) \right] \epsilon^{j(\omega t - \beta z)}$$

Region 2

$$E_{2z} = C_2 H_o^{(1)} (h_2 \rho) \epsilon^{j(\omega t - \beta z)}$$

$$E_{2\rho} = \frac{-j\beta}{\sqrt{K_2^2 - \beta^2}} C_2 H_1^{(2)} (h_2 \rho) \epsilon^{j(\omega t - \beta z)} \qquad (11)$$

$$H_{2\theta} = \frac{-jK_2^2}{\omega\mu_2 \sqrt{K_2^2 - \beta^2}} C_2 H_1^{(1)} (h_2 \rho) \epsilon^{j(\omega t - \beta z)}$$

In order to find the eigen values of the problem and the values of the coefficients A_1, B_1, and C_2, we make recourse to the following boundary conditions:

$$\rho = a, \quad E_{1z} = 0$$

$$\rho = b, \quad E_{1z} = E_{2z}, \; H_{1\theta} = H_{2\theta} \qquad (12)$$

From the first condition, we obtain

$$A_1 J_o (h_1 a) + B_1 N_o (h_1 a) = 0 \qquad (13)$$

i.e.,

$$B_1 = -A_1 \frac{J_o (h_1 a)}{N_o (h_1 a)} \qquad (14)$$

Substituting in Equa. 10, we obtain:

$$E_{1z} = A_1 \left[J_o (h_1 \rho) \; N_o (h_1 a) - J_o (h_1 a) \; N_o (h_1 \rho) \right] \epsilon^{j(\omega t - \beta z)}$$

$$E_{1\rho} = \frac{-j\beta A_1}{h_1} \left[J_1 (h_1\rho) \; N_o (h_1 a) - J_o (h_1 a) \; N_1 (h_1 \rho) \right] \times \epsilon^{j(\omega t - \beta z)} \tag{15}$$

$$H_{1\theta} = \frac{jK_1^2}{\omega \mu_1 h_1} A_1 \left[J_1 (h_1\rho) \; N_o (h_1 a) - J_o (h_1 a) \; N_1 (h_1 \rho) \right] \times \epsilon^{j(\omega t - \beta z)}$$

Turning now to the boundary condition at $\rho = b$, we write:

$$A_1 \left[J_o (h_1 b) \; N_o (h_1 a) - J_o (h_1 a) \; N_o (h_1 b) \right] = C_2 H_o^{(1)} (h_2 b)$$

$$\frac{K_1^2}{\omega_1 h_1 \mu_1} A_1 \left[J_1 (h_1 b) \; N_o (h_1 a) - J_o (h_1 a) \; N_1 (h_1 b) \right] = \frac{K_2^2 \, C_2}{\omega \mu_2 h_2} H_1^{(1)} (h_2 b) \tag{16}$$

In order to solve the above system of equations, we introduce the following substitutions:

$$h_1 b = u \,, \quad h_2 b = v$$

$$h_1 a = us \,, \quad h_2 a = vs \tag{17}$$

Where $s = a/b$. Hence, Equa. 16 may be written as follows:

$$A_1 \left[J_o(u) \; N_o(us) - J_o(us) \; N_o(u) \right] = C_2 H_o^{(1)} (v)$$

$$\frac{K_1^2}{\omega \mu_1 h_1} A_1 \left[J_1(u) \; N_o(us) - J_o(us) \; N_1(u) \right] = \frac{K_2^2}{\omega \mu_2 h_2} C_2 H_1^{(1)} (v) \tag{18}$$

Since the above system of equations is homogeneous, necessary and sufficient condition for the existence of a non-trivial solution is:

$$\frac{J_1(u)\ N_o(us) - J_o(us)\ N_1(u)}{J_o(u)\ N_o(us) - J_o(us)\ N_o(u)}\ \frac{K_1^{\ 2}\ \mu_2 h_2}{K_2^{\ 2}\ \mu_1 h_1} - \frac{H_1^{(1)}(v)}{H_o^{(1)}(v)} = 0 \qquad (19)$$

An equivalent expression of Equa. 22 is written as follows:

$$\frac{\epsilon_1}{u\ \epsilon_2}\ \frac{J_1(u)\ \ N_o(us) - J_o(us)\ \ N_1(u)}{J_o(u)\ \ N_o(us) - J_o(us)\ \ N_o(u)} - \frac{1}{v}\ \frac{H_1(v)}{H_o(v)} = 0 \qquad (20)$$

If the quantities u and v are very small, as in the case of interest for the present investigations, Equa. 20 can be simplified noting that;

$$H_o(v) \cong \frac{2j}{\pi} \ln \frac{\gamma v}{2j}$$

$$H_1(v) = -\ 2j/\pi v$$

$$J_o(u) \cong 1,\ J_1(u) \cong 0 \qquad (21)$$

$$N_o(u) \cong \frac{2}{\pi} \ln \frac{2}{\gamma u}$$

$$N_1(u) \cong 2/\pi u$$

where $\gamma = 1.781$.

Substituting into Equa. 20, one has finally:

$$-\frac{\epsilon_1}{\epsilon_2}\ \frac{1}{u^2 \ln \frac{1}{s}} + \frac{1}{v^2 \ln \frac{v}{2j}} = 0 \qquad (22)$$

i.e., letting $\epsilon_1/\epsilon_2 = \epsilon$:

TABLE OF CONTENTS

		PAGE
1.	INTRODUCTION	1
2.	THEORY OF FERRITE-LOADED RADIATORS	2
3.	INITIAL PROPOSAL OF FERRITE-LOADED OMEGA ANTENNA DESIGN	17
4.	REVIEW OF EXISTING VLF ANTENNA SYSTEMS	21
5.	RADIATION RESISTANCE OF VLF ANTENNAS	28
6.	DESIGN OF THE GROUND PLANE	29
7.	DESIGN OF THE TOP LOAD	36
8.	EXPERIMENTAL VERIFICATION OF LOW-FREQUENCY FERRITE ANTENNA DESIGN	38
9.	CONCLUSIVE REMARKS	41

CONFIDENTIAL

LIST OF FIGURES

FIGURE		PAGE
1	Cylindrical Coordinate System	14
2	Plots of Equations 29 and 30	15
3	Wavelength Reduction for Infinite Ferrite-Loaded Line	16
4	Preliminary Proposal of Omega Ferrite Antenna	
5	Alternate Preliminary Proposal of Omega Ferrite Antenna	
6	Jim Creek VLF Transmitting Antenna	
7	Diagram of the Annapolis, Md., Antenna	
8	Rocky Point Antenna	
9	Rugby GBR Transmitting Antenna	
10	Rugby GBR Transmitting Antenna Ground System	
11	Diagram of the Marion, Mass., and New Brunswick, N.J., VLF Transmitting Antennas	
12	Diagram of the VLF Antenna at Tuckerton, N.J.	
13	Examples of Top-Loaded Antennas	
14	Theoretical and Experimental Values of Radiation Resistance versus H/λ	
15	Experimental Values of R_r for Various Ferrite-Loaded Antennas versus H/λ	
16	Phase and Density of Radial Ground Current	
17	Sketch of Antenna System	
18	Optimum and Terminal Spacing of Buried Conductors	
19	ΔR and ΔX vs r_t/λ $(h/\lambda = 0.25)$	
20	ΔR and ΔX vs r_t/λ $(h/\lambda = 0.1$ and $0.01)$	
21	ΔR and ΔX vs r_t/λ (Parameter a/λ)	
22	ΔR and ΔX vs a/λ (Parameter r_t/λ)	
23	ΔR vs α/π	
24	ΔR vs h/λ $(\alpha = \pi/2$ or $0)$	
25	ΔR and ΔX vs r_t/λ for Various Surface Impedance Values	
26	Relationship between δ and Ground Conductivity	
27	Assumed Antenna Current Distribution	
28	Radial Density Component J_ρ^v vs ρ/h	
29	Surface Current Density J_s^h vs ρ/h at Two Azimuths $(h/\lambda = 0)$	
30	Surface Current Density J_s^h vs ρ/h at Two Azimuths $(h/\lambda = 0.06)$	

CONFIDENTIAL

31	L- and T-Type Loading
32	Ratio $J_{\phi}^{h}/J_{\varphi}^{v}$ for L-Type Loading
33	Ratio $J_{\phi}^{h}/J_{\varphi}^{v}$ for T-Type Loading $(h/\lambda = 0)$
34	Wavelength Shortening Ratio of 3" Ferrite Radiator vs Length
35	Input Resistance and Reactance of 100-Ft Ferrite Radiator
36	Radiation Pattern of 100' Ferrite Antenna

LIST OF TABLES

TABLE		PAGE
I	SUMMARY OF PROPERTIES OF FERRITE TOROIDS USED	12
II	RESONANT FERRITE MONOPOLES	13
III	SUMMARY OF VLF ANTENNA CHARACTERISTICS	27

FEASIBILITY OF DESIGN OF OMEGA ANTENNAS BY FERRITE-LOADING TECHNIQUES

1. INTRODUCTION

The following Technical Report represents a summary of a theoretical and experimental investigation conducted under Contract NOnr 3358, NR 373-804 during the period January 1964 to May 1965, in order to verify and extend the calculations developed previously, under the same contract, for the design of an Omega Transmitting system, using ferrite-loading techniques. The data presented in the following report include some results obtained in the investigation of a ferrite-loaded Low Frequency transportable-type antenna.

Ferrite-loading techniques for transmitting antennas have been investigated extensively at ITT FEDERAL LABORATORIES under Contract NOnr 3358 for application to the design of VLF, LF, and HF radiators. In a previous Technical Report entitled "VLF Ferrite Antennas", dated November 1963, the theoretical analysis of linear loading was developed; in particular, the axial wavelength shortening ratio λ_z/λ_o, the height-to-air-wavelength ratio H/λ_o, the relative bandwidth, the radiation resistance and the radiation efficiency, the proximity interaction between unloaded and loaded conductors, etc., were studied. Experimental verifications conducted at H.F. (2 to 26 mc/s) provided excellent agreement with the theoretical calculations.

On the basis of these results, a design of transmitting antenna system for Omega application was developed. This consisted of a cage-type structure built with 500' ferrite-loaded monopoles, supported by means of 500' or 650' towers. The details of this design are summarized in a following Section. Extrapolating results obtained at HF, the principal characteristics of the antenna system such as resonance wavelength for

given ferrite loading, radiation resistance, maximum radiated power, etc., were derived.

In order to provide a check of the validity of the extrapolation, an experimental investigation of a low-frequency antenna representing approximately a 10-to-1 model of the proposed Omega system was undertaken. The Federal Communications Commission granted ITT FEDERAL LABORATORIES an experimental Radio Station License for operation at 81.7 Kc/s and 69 Kc/s, with a maximum radiated power of 5000 watts. After a thorough study of ground-plane techniques and requirements, a site was selected at Nutley, N.J., and a 100'-high vertical monopole using ferrite-loading techniques was built. Permission for the erection of the required 100' towers was granted by the Federal Aviation Agency. Although, at the date of the writing of the present report, the investigation of the properties of this transmitting system has not yet been completed, a wealth of experimental results of great technical significance has been already obtained. These are presented in the following, along with conclusions and recommendations for application to the final Omega system design.

2. THEORY OF FERRITE-LOADED RADIATORS

The theory of linear ferrite-loaded antennas may be developed from consideration of an infinite cylindrical wire of diameter $2a$ coated with a uniform sheath of ferrite of diameter $2b$ (Fig. 1).

Consider an infinite straight conductor of infinite conductivity and radius a, surrounded by an uniform ferrite cylinder of inner radius a, and outer radius b, having permeability μ, and permittivity ϵ_1. Using a cylindrical coordinate system ρ, θ, z, one finds that the electromagnetic field distribution may be expressed in terms of two Hertz vector potentials π_1 and π_2 both parallel to the z axis and such that their magnitudes satisfy the scalar wave equation:

$$\nabla^2 - \mu\epsilon \frac{\delta^2}{\delta t^2} - \mu \frac{\delta}{\delta t} \psi = 0 \tag{1}$$

Assuming harmonic time and space dependence, one may let, in general:

$$\psi = f(\rho, \theta) \exp(j\omega t - \beta z) \tag{2}$$

where $f(\rho\theta)$ is a solution of the equation

$$\frac{1}{\rho}\frac{\delta}{\delta\rho}\left(\rho\frac{\delta f}{\delta\rho}\right)+\frac{1}{\rho^2}\frac{\delta^2 f}{\delta\theta^2}+(K^2-\beta^2)f=0 \qquad (3)$$

In the above equation, the coefficient K is expressed in terms of the characteristics of the medium; i.e.,

$$K^2=\omega^2-j\omega\mu\sigma \qquad (4)$$

and the coefficient β is the axial propagation constant; i.e.,

$$\beta = 2\pi/\lambda_z \qquad (5)$$

where λ_z is the wavelength along the z axis. The general expression of the electromagnetic field is derived from the vector potentials π_1 and π_2, using the following relations:

$$\bar{E} = \nabla\times\nabla\times\overline{\pi_1}+j\omega\mu\nabla\times\overline{\pi_2} \qquad (6)$$

$$\bar{H} = (\sigma+j\omega\epsilon)\overline{\pi_1}+\nabla\times\nabla\times\overline{\pi_2}$$

It is seen that the field derived from $\overline{\pi_1}$ has no axial magnetic field component, while the field derived from $\overline{\pi_2}$ has no axial electric field component; for this reason, the two field configurations are called respectively "transverse magnetic" and "transverse electric".

Clearly, the problem of interest in the present investigation falls into the class of transverse magnetic modes. We can proceed accordingly, neglecting $\overline{\pi_2}$ and solving Eq. 3 separately in region 1, (i.e., $a \leq \rho \leq b$), and in region 2 (i.e., $b \leq \rho \leq \infty$).

In region 1, we may let, in general,

$$E_{1z} = \sum_{n=0}^{\infty} \left[(A_{1n} J_n (h_{1n} \rho) + B_{1n} N_n (h_{1n} \rho)\right] \epsilon^{j(n\theta + \omega t - \beta_n z)} \quad (7)$$

$$H_{1z} = 0$$

and in region 2, we may let

$$E_{2z} = \sum_{n=0}^{\infty} C_{2n} \; H_n^{(1)} (h_{2n} \rho) \; \epsilon^{j(n\theta + \omega t - \beta_n z)} \quad (8)$$

In the above equations,

$$h_{1n}^2 = K_1^2 - \beta_n^2 \quad (9)$$

$$h_{2n}^2 = K_2^2 - \beta_n^2$$

Since we are interested in fields which are distributed uniformly with respect to the angle θ, we shall limit our investigation to the zero-order mode only; i.e., $n = 0$. Hence, applying Equa. 7, we find:

Region 1

$$E_{1z} = \left[A_1 J_o (h_1 \rho) + B_1 N_o (h_1 \rho)\right] \epsilon^{j(\omega t - \beta z)} \quad (10)$$

$$E_{1\rho} = \frac{-j\beta}{\sqrt{K_1^2 - \beta^2}} \left[A_1 J_1 (h_1 \rho) + B_1 N_1 (h_1 \rho)\right] \epsilon^{j(\omega t - \beta z)}$$

$$H_{1\theta} = \frac{-jK_1^2}{\omega \mu_1 \sqrt{K_1^2 - \beta^2}} \left[A_1 J_1 (h_1 \rho) + B_1 N_1 (h_1 \rho)\right] \epsilon^{j(\omega t - \beta z)}$$

Region 2

$$E_{2z} = C_2 H_o^{(1)} (h_2 \rho)\, \epsilon^{j(\omega t - \beta z)}$$

$$E_{2\rho} = \frac{-j\beta}{\sqrt{K_2^2 - \beta^2}}\, C_2 H_1^{(2)} (h_2 \rho)\, \epsilon^{j(\omega t - \beta z)} \tag{11}$$

$$H_{2\theta} = \frac{-jK_2^2}{\omega\mu_2 \sqrt{K_2^2 - \beta^2}}\, C_2 H_1^{(1)} (h_2 \rho)\, \epsilon^{j(\omega t - \beta z)}$$

In order to find the eigen values of the problem and the values of the coefficients A_1, B_1, and C_2, we make recourse to the following boundary conditions:

$$\rho = a, \quad E_{1z} = 0$$

$$\rho = b, \quad E_{1z} = E_{2z}, \; H_{1\theta} = H_{2\theta} \tag{12}$$

From the first condition, we obtain

$$A_1 J_o (h_1 a) + B_1 N_o (h_1 a) = 0 \tag{13}$$

i.e.,

$$B_1 = -A_1 \frac{J_o (h_1 a)}{N_o (h_1 a)} \tag{14}$$

Substituting in Equa. 10, we obtain:

$$E_{1z} = A_1 \left| J_o(h_1\rho) \; N_o(h_1a) - J_o(h_1a) \; N_o(h_1\rho) \right| \epsilon^{j(\omega t - \beta z)}$$

$$E_{1\rho} = \frac{-j\beta A_1}{h_1} \left[J_1(h_1\rho) \; N_o(h_1a) - J_o(h_1a) \; N_1(h_1\rho) \right] \times \epsilon^{j(\omega t - \beta z)} \qquad (15)$$

$$H_{1\theta} = \frac{jK_1^{\,2}}{\omega \mu_1 h_1} A_1 \left[J_1(h_1\rho) \; N_o(h_1a) - J_o(h_1a) \; N_1(h_1\rho) \right] \times \epsilon^{j(\omega t - \beta z)}$$

Turning now to the boundary condition at $\rho = b$, we write:

$$A_1 \left[J_o(h_1b) \; N_o(h_1a) - J_o(h_1a) \; N_o(h_1b) \right] = C_2 H_o^{(1)}(h_2b)$$

$$\frac{K_1^{\,2}}{\omega_1 h_1 \mu_1} A_1 \left[J_1(h_1b) \; N_o(h_1a) - J_o(h_1a) \; N_1(h_1b) \right] = \frac{K_2^{\,2} \; C_2}{\omega \mu_2 h_2} H_1^{(1)}(h_2b) \qquad (16)$$

In order to solve the above system of equations, we introduce the following substitutions:

$$h_1b = u \; , \quad h_2b = v$$

$$h_1a = us \; , \quad h_2a = vs \qquad (17)$$

where $s = a/b$. Hence, Equa. 16 may be written as follows:

$$A_1 \left[J_o(u) \; N_o(us) - J_o(us) \; N_o(u) \right] = C_2 H_o^{(1)}(v)$$

$$\frac{K_1^{\,2}}{\omega \mu_1 h_1} A_1 \left[J_1(u) \; N_o(us) - J_o(us) \; N_1(u) \right] = \frac{K_2^{\,2}}{\omega \mu_2 h_2} C_2 H_1^{(1)}(v) \qquad (18)$$

Since the above system of equations is homogeneous, necessary and sufficient condition for the existence of a non-trivial solution is:

$$\frac{J_1(u)\ N_o(us) - J_o(us)\ N_1(u)}{J_o(u)\ N_o(us) - J_o(us)\ N_o(u)}\ \frac{K_1^{\ 2}\ \mu_2 h_2}{K_2^{\ 2}\ \mu_1 h_1} - \frac{H_1^{(1)}(v)}{H_o^{(1)}(v)} = 0 \qquad (19)$$

An equivalent expression of Equa. 22 is written as follows:

$$\frac{\epsilon_1}{u\ \epsilon_2}\ \frac{J_1(u)\ \ N_o(us) - J_o(us)\ \ N_1(u)}{J_o(u)\ \ N_o(us) - J_o(us)\ \ N_o(u)} - \frac{1}{v}\ \frac{H_1(v)}{H_o(v)} = 0 \qquad (20)$$

If the quantities u and v are very small, as in the case of interest for the present investigations, Equa. 20 can be simplified noting that;

$$H_o(v) \cong \frac{2j}{\pi}\ \ln \frac{\gamma v}{2j}$$

$$H_1(v) = -\ 2j/\pi v$$

$$J_o(u) \cong 1, \quad J_1(u) \cong 0 \qquad (21)$$

$$N_o(u) \cong \frac{2}{\pi}\ \ln \frac{2}{\gamma u}$$

$$N_1(u) \cong 2/\pi u$$

where $\gamma = 1.781$.

Substituting into Equa. 20 , one has finally:

$$-\ \frac{\epsilon_1}{\epsilon_2}\ \frac{1}{u^2 \ln \frac{1}{s}} + \frac{1}{v^2 \ln \frac{v}{2j}} = 0 \qquad (22)$$

i.e., letting $\epsilon_1/\epsilon_2 = \epsilon$:

$$\epsilon\, v^2\, \ell n\, \frac{\gamma v}{2j} = u^2\, \ell n\, (1/s) \tag{23}$$

In order to remove the imaginary, it is convenient to define a new set of variables; i.e.,

$$u = p = h_1 b$$
$$v = jq = h_2 b \tag{24}$$

In terms of p and q , Equas. 9 and 23 are written as follows:

$$K_1^2 - \beta^2 = p^2/b^2$$
$$K_2^2 - \beta^2 = -q^2/b^2 \tag{25}$$
$$\epsilon\, q^2\, \ell n\, \frac{2}{\gamma q} = p^2\, \ell n\, (b/a)$$

Up to this point, we have assumed that the conductivity of the ferrite is greater than zero. In practice, however, we may expect to use a low-loss ferrite material and correspondingly may let $\sigma = 0$. There follows:

$$K_2^2 = \omega^2 \mu_2 \epsilon_2 = (2\pi / \lambda_o)^2$$
$$K_1^2 = \omega^2 \mu_1 \epsilon_1 = (2\pi / \lambda_o)^2 \mu\epsilon \tag{26}$$

where $\mu = \mu_1/\mu_2$, $\epsilon = \epsilon_1/\epsilon_2$. Substituting in Equa. 25 and manipulating, one finds:

$$\left(\frac{2\pi}{\lambda_o}\right)^2 \mu\epsilon - \left(\frac{2\pi}{\lambda_z}\right)^2 = p^2/b^2$$
$$\left(\frac{2\pi}{\lambda_o}\right)^2 - \left(\frac{2\pi}{\lambda_z}\right)^2 = q^2/b^2 \tag{27}$$
$$\epsilon q^2\, \ell n\, \frac{2}{\gamma s} = p^2\, \ell n\, s$$

Finally, adding and subtracting the first two equations of 27, one obtains:

$$\frac{2\pi b}{\lambda_o} = \frac{\sqrt{p^2+q^2}}{\sqrt{\epsilon\mu - 1}}$$

$$\lambda_z/\lambda_o = \frac{\sqrt{p^2+q^2}}{\sqrt{p^2+\epsilon\mu q^2}} \qquad (28)$$

$$p^2 \ln \frac{b}{a} = \epsilon q^2 \ln \frac{1.12}{q}$$

The above system of equations provides the solution of the problem of the design of a resonant ferrite antenna. Given the values of ϵ and μ for the ferrite material and of the radii a and b, the ratio λ_z/λ_o is computed. Alternatively, given ϵ, μ, and λ_z/λ_o, one can find the required values of a and b for which the desired wavelength reduction is obtained.

The information contained in Equa. 28 may be presented in graphical form in a number of ways. From the first of Equa. 28, it is seen that a family of circles for constant λ_o/b is described with the equation:

$$p^2 + q^2 = (\epsilon\mu - 1)\ (2\pi b/\lambda_o)^2 \qquad (29)$$

On the other hand, the equation

$$p^2 \ln (b/a) = \epsilon q^2 \ln (1.12/q) \qquad (30)$$

describes a family of curves, each characterized by a given ratio b/a. The families corresponding to Eq. 29 and 30 are plotted in Fig. 2 for a given type of ferrite having relative average permeability $\mu = 100$ and relative average permittivity $\epsilon = 10$. Using the latter diagram, it is possible to find the values of the quantities p and q which correspond to a given set of values λ_o/b and b/a. Substituting in the equation:

$$\frac{\lambda_z}{\lambda_o} = \sqrt{\frac{p^2 + q^2}{p^2 + \mu \epsilon q^2}} \qquad (3\cdot)$$

the desired ratio λ_z/λ_o is computed. It is of interest to note that, in certain ranges of the variables λ_o/b and b/a, two solutions are obtained; for instance, letting $\lambda_o/b = 100$ and $b/a = 5$, one finds:

$$p = 1.2, \quad q = 0.7, \quad \lambda_z/\lambda_o = 0.0625$$
$$p = 1.09, \quad q = 0.87, \quad \lambda_z/\lambda_o = 0.0509 \qquad (32)$$

The maximum permissible value of q is 1.12 ; this corresponds to $\lambda_o/b = 177$ and to $p = 0$. In this case, one finds $\lambda_z/\lambda_o = 1/\sqrt{\mu\epsilon}$ regardless of the ratio b/a. Associated with the same ratio λ_z/b, there is found also another solution for each value of b/a.

In experimental verifications, the degeneracy above illustrated is not found, and only the solutions corresponding to the smaller of the q values is obtained. The result may be attributed to the occurrence of additional boundary conditions not included in the above analysis.

A more compact representation of the design equations 28 is obtained eliminating the quantity p; in fact, solving the first equation in terms of p, one has:

$$p^2 = (\epsilon \mu - 1) \left(\frac{2\pi b}{\lambda_o}\right)^2 - q^2 \qquad (33)$$

Substituting in the remaining equations, these acquire the following form:

$$\lambda_z/\lambda_o = 1/\sqrt{1 + \frac{\lambda_o}{2\pi b} q^2}$$
$$(\epsilon \mu - 1) \left(\frac{2\pi b}{\lambda_o}\right)^2 = q^2 \left[1 + (\ln 1.12 - \ln q)/\ln \frac{b}{a} \right] \qquad (34)$$

From the latter expressions it is noted that, for a given value of the ratio λ_o/b, the ratio λ_z/λ_o becomes smaller, the larger is the value of the parameter q. The parameter q is obtained as a solution of the second equation of 34. Although the latter equation is of transcendental form (and for this reason cannot be analyzed directly), some considerations of a qualitative nature may be derived. Assume, for example, that q is very small with respect to unity. In this case, the said equation reduces approximately to the following form:

$$(\epsilon\,\mu - 1)\;\;(2\pi\, b/\lambda_o)^2 = -q^2\,\ell n\, q/\ell n\,\frac{b}{a} \tag{35}$$

The function $q^2\ell nq$ is zero at $q = 0$ and increases monotonically with the increase of q; hence, q increases with $\ell n\frac{b}{a}$, $(\epsilon\,\mu - 1)$ and b/λ_o. Quantitative values are obtained plotting the variable λ_z/λ_o as a function of λ_o/b for given values of the ratio b/a and for a given type of ferrite material. An example is shown in Fig. 3, computed for a ferrite material of characteristics $\epsilon = 10$, $\mu = 100$, and for b/a values of 1.5, 3, 3.5, 10, 25, and 100.

The above theoretical results provide information about the axial wavelength shortening of the ferrite-loaded antenna. This property has also been tested experimentally and found to be in excellent agreement with the theory. As an example, measurements of resonance, radiation efficiency, and bandwidth of vertical ferrite-loaded monopoles are summarized in Table I, where ferrites A, B, and C have the characteristics and dimensions shown in Table II. It is noted that, in the case of Type A ferrite-loading, the ratio H/λ_o is 0.05 at 25.9 mc/s, and 0.075 at 1.89 mc/s; the relative bandwidth is of the order of 3%, the input impedance of the order of 12 ohms, and the radiation resistance is of the order of 5 ohms. The above experimental results are in agreement with the theoretical results of Fig. 3, for the case $b/a = 1.67$.

TABLE I

SUMMARY OF PROPERTIES OF FERRITE TOROIDS USED

	TYPE A	TYPE B	TYPE C	TYPE D
μ_r	100	100	100	100
ϵ_r	10	10	10	10
Loss Factor = $\frac{1}{\mu_o Q}$ at 1 Mc	.00002	.00002	.00002	.00002
at 10 Mc	.00016	.00016	.00016	.00016
Sat. Flux Density B_{max} (gauss)	3300	3300	3300	3300
Curie Point °C	350	350	350	350
Inner Radius "a" (cm)	0.95	1.75	0.218	0.316
Outer Radius "b" (cm)	1.59	2.38	1.27	7.62

TABLE II

RESONANT FERRITE MONOPOLES

HEIGHT (Ft.)	FERRITE TYPE	RESON. FREQ. (Mc)	H/λ_o	Z_{in} (Ohms)	EFF. (%)	BW (Kc)	BW (%)
2	A	25.9	0.05	50	10	-	-
4	A	14.1	0.06	12	24	950	6.75
8	A	7.34	0.06	12	47	240	3.3
16	A	3.72	0.06	12	37	100	2.7
40	A	1.89	0.075	-	-	-	-
4	C	8.50	0.034	28	4.6	-	-
4	A & B	11.4	0.046	12	17	-	-

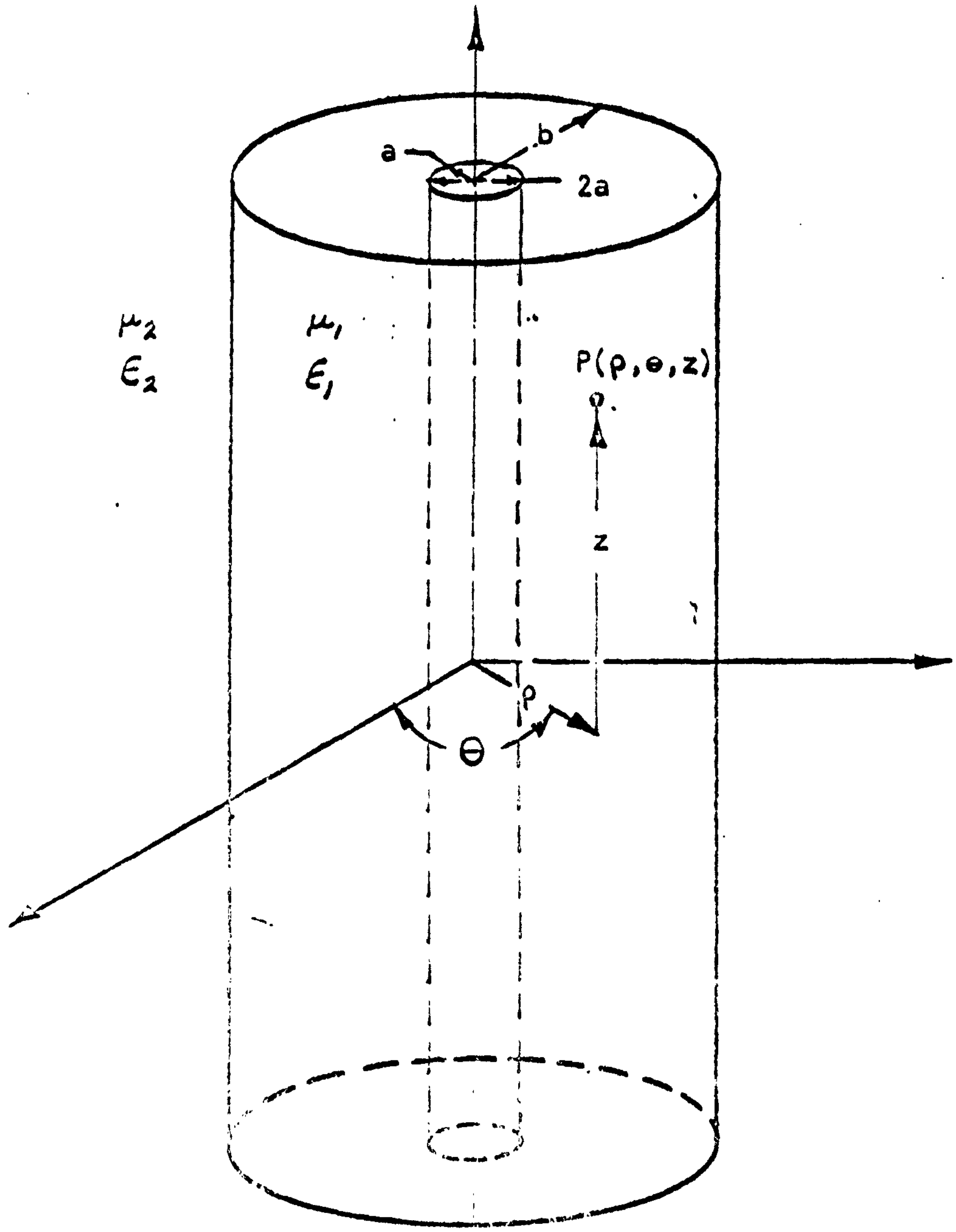

FIGURE 1
CYLINDRICAL COORDINATE SYSTEM

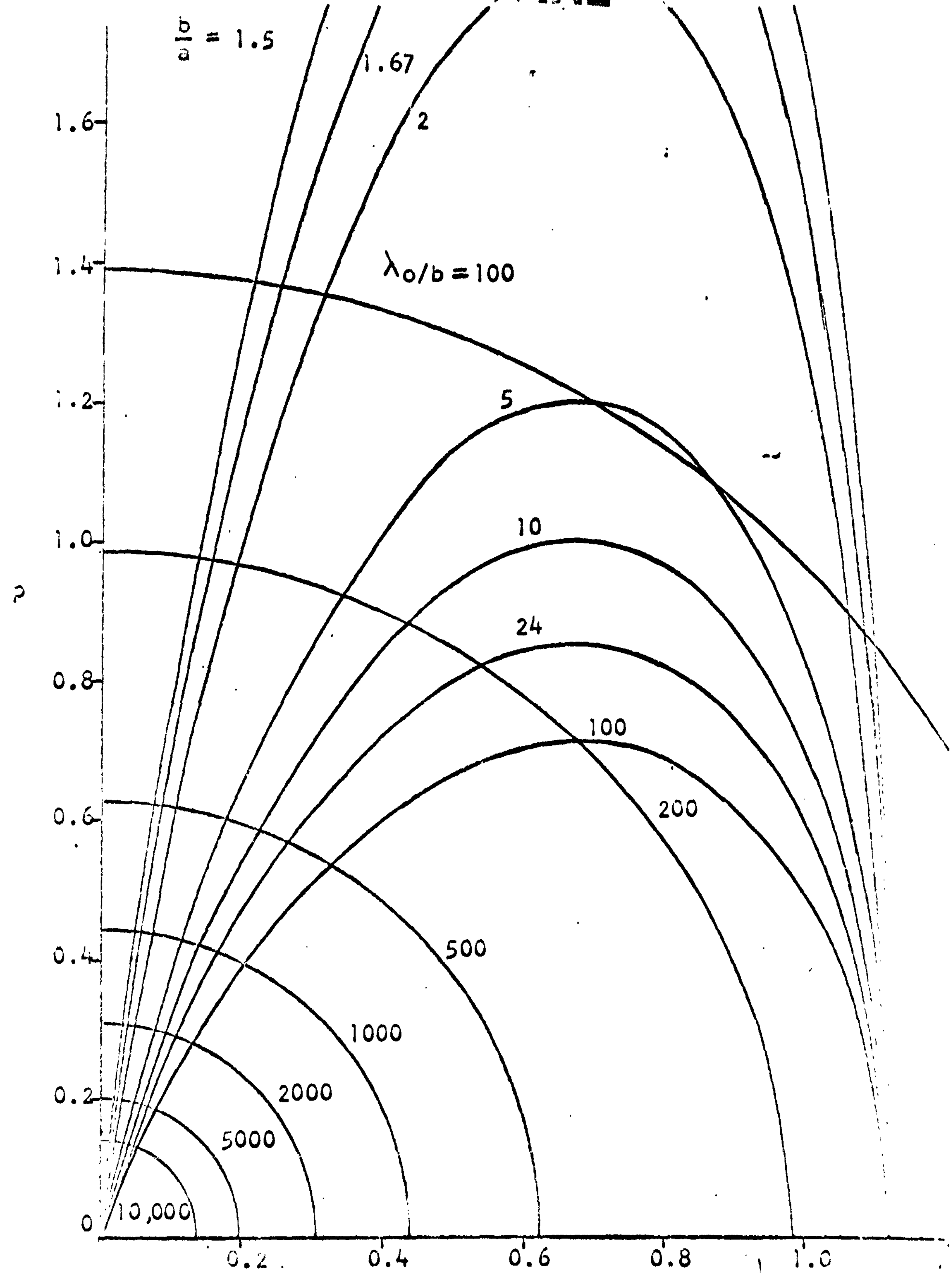

FIGURE 2-PLOTS OF EQUATIONS 29 AND 30

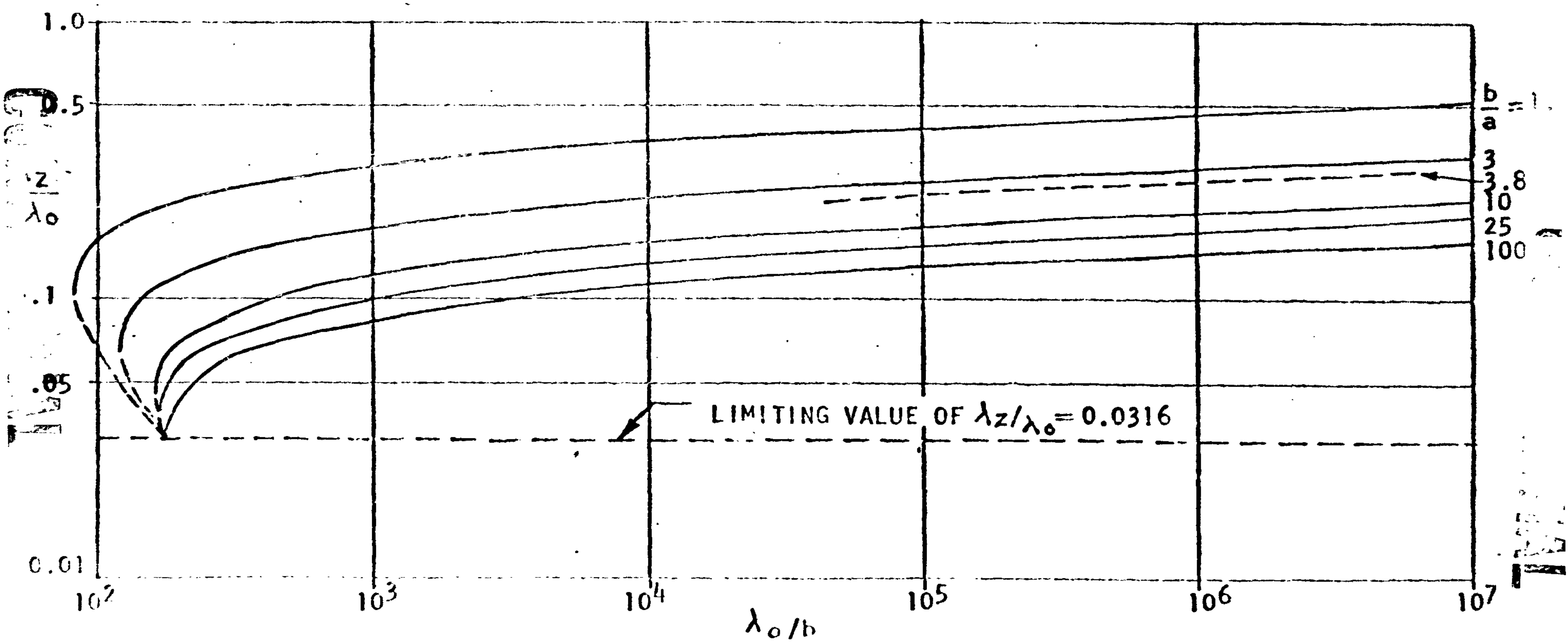

FIGURE 3.- WAVELENGTH REDUCTION FOR INFINITE FERRITE LOADED LINE

3. INITIAL PROPOSAL OF FERRITE-LOADED OMEGA ANTENNA DESIGN

For purposes of reference, it is useful to summarize and review the initial proposal of design of the Ferrite-loaded Omega Antenna System developed at ITT FEDERAL LABORATORIES in November 1963.

The general layout of the antenna system is shown in Fig. 4 and in Fig. 5 for two configurations, differing in the manner of support of the ferrite radiators; in the case of Fig. 4, the radiators are supported by means of longitudinal steel ropes which are spanned between steel towers 650-ft high and 580-ft apart; and in the case of Fig. 5, the radiators are attached directly to steel towers each 500-ft high.

The ferrite material selected for this application has the following characteristics:

Inner Radius	= $a = 0.95$ cm (0.375 in.)
Outer Radius	= $b = 3.8$ cm (1.5 in.)
Permeability	$\mu_{min} = 100$, $\mu_{max} = 400$
Permittivity	$\epsilon = 10$
Curie Point	350°C
Loss Factor	$\frac{1}{\mu Q} = 2 \times 10^{-5}$
Density	4.5 g/cm^3
Saturation Flux Density	3500 gauss

Using the equations derived in the previous Section, and, in particular, using the family of curves of Fig. 3, one may compute the theoretical axial resonance wavelength of the antenna. The parameters λ_o/b and b/a are respectively 7.9×10^5 and 3.8 ; there follows that the ratio of the axial wavelength λ_z to the free space wavelength is:

$$\lambda_z/\lambda_o = 0.27 \qquad (36)$$

At $f = 10.2$ Kc, one has $\lambda_o = 29,400$ m and $\lambda_z = 7,940$ m; a quarter-wavelength is therefore $\lambda_z/4 = 1,980$ m and, using an actual radiator

height of 500 ft = 152 m, the ratio H/λ_o is 5.16×10^{-3}. The radiation resistance is a function of top loading; assuming a value

$$R_{rad} = 0.10 \text{ ohm} \tag{37}$$

and assuming a maximum base antenna current of 100 A (rms), the maximum radiated power per antenna is:

$$P_r = R_{rad} I^2 = 1000 \text{ watt} \tag{38}$$

The maximum permissible antenna current depends upon the magnetic saturation of the ferrite and upon its Curie temperature. Since $B_{sat} = 3500$ gauss $= 0.35 \text{ Wh/m}^2$, there follows:

$$H_{sat} = B_{sat}/\mu\mu_o = \frac{0.35}{4\pi} 10^5 = 2,780 \text{ A/m} \tag{39}$$

In the latter equation, an approximate value $\mu = 100$ has been used. The corresponding value of maximum current is:

$$I_{max} = 2\pi \, a \, H_{sat} = 166 \text{ A} \tag{40}$$

The current limitation due to maximum operating temperature cannot be computed theoretically since the value depends upon the loss resistance of the ferrite and of other radiator elements and upon the effective values of thermal coefficients of the system in air; however, since the frequency of operation is low and the Curie temperature is high, it is reasonable to conclude that the upper limit of antenna current corresponding to operation at a temperature near the Curie value is well above the limit represented by Equation 40.

The proposed antenna system consists of a cage structure with nine radiator elements. Assuming that the interaction between radiators is negligible, the total maximum radiated power is:

$$P_{rad} = R_r (9I)^2 = 81 \text{ kw} \tag{41}$$

In practice, the interaction may be expected to result in an increase of the effective value of λ_z/λ_o ; on the basis of experimental studies at HF, the latter increase is estimated to be of the order of 20%; i.e., the effective value of λ_z/λ_o would increase from 0.27 to 0.32 . This would result in a decrease of the radiation resistance from 0.10 to 0.085 and, therefore, in a decrease of the radiated power from 81 kw to 68.5 kw . However, the radiation resistance depends upon the top loading of the system, so that a compensation of the decrease may be realized with a suitable increase of the top loading. This matter is discussed in detail in a following Section.

An important characteristic of the antenna system is its bandwidth; this cannot be predicted accurately because it depends upon the variation of the input reactance for the cage structure. However, experimental investigations conducted at HF have shown that bandwidth values well in excess of 3% are realizable.

Another parameter of interest is the radiative efficiency; this is expressed as the ratio:

$$\eta_{rad} = R_r / (R_r + R_{loss}) \tag{42}$$

and, therefore, depends directly upon the loss resistance. An exact estimate of the latter cannot be given at the present time; the loss contribution of the ground plane may be reduced well below 1 ohm and that of the ferrite material is known to be very low at 10.2 kc . Losses are contributed by the steel towers which are used to support the radiators and by the insulators, guy wires, etc.

With careful engineering design, the over-all loss resistance should be maintained of the order of 1 ohm ; this would result in a radiation efficiency of the order of 10% .

As far as the mechanical design of the systems shown in Figs. 4 and 5 is concerned, the towers may be of guyed type; the ferrite radiators

use an axial conductor consisting of a steel rope of diameter 0.5" with copper bushings of diameter 0.75", on which the ferrite toroids (ID.= 0.75", O.D. = 3") are mounted. Each 500-ft radiator weighs 7,285 lbs, calculated as follows:

Ferrite material	6,640 lbs.
Steel rope (0.39 lb/ft)	195 "
Steel and Copper Sleeves	450 "
	7,285 lbs.

Selecting a 6 x 37 flexible hoisting-type steel rope having a breaking strength of 20,400 lbs., a safety factor of 20,400/7,285 = 2.8 is obtained.

In the case of Fig. 4, the horizontal supporting ropes have diameter 5/8" and a breaking strength of 31,600 lbs. Suitable pulley systems are considered for hoisting and supporting the radiators.

In the case of Fig. 5, the design of the towers and that of the supports of the radiators are simplified; the radiators are mounted along the axis of each tower with suitable insulated supports. The proximity effect of the steel towers is not expected to affect the radiation resistance, but may affect the loss resistance; a thorough evaluation of the phenomena involved has not been made.

The total area covered by the cage structures of Fig. 4 and of Fig. 5 is approximately 140 acres . In the actual design, the area may have to be increased to include suitable top loading; the area of the ground plane is comparable with that of various other antenna installations.

4. REVIEW OF EXISTING VLF ANTENNA SYSTEMS

For purposes of comparative evaluation, it is useful to summarize the principal characteristics of existing VLF antenna systems. The following installations have been studied: Cutler, Forestport, Jim Creek, Annapolis, Lualualei, Rocky Point, Rugby, Haiku, New Brunswick, Canal Zone, Marion, Tuckerton.

The Cutler Antenna, part of the Navy VLF transmitting station located in Cutler, Maine, consists of two arrays whose centers are separated by one mile and which may be operated independently or in dual. Each array has a mean height of 848 ft. and a radius of 3070 ft.; it consists of one center tower of 980 ft. and 12 smaller towers ranging from 875 to 800 ft., which support its star-shaped top hat.

The top hat of each array is made up of six independent diamond sections which are insulated from the towers and can be controlled separately; that is, they can be lowered or raised for repairs or for prevention of damage from heavy icing. A unique arrangement of the RF feed lines makes it possible to pass 60-cycle deicing currents through either array to remove ice under moderate icing conditions. Since the arrays may be operated independently, this arrangement allows one array to continue transmitting while the other is being deiced; hence, the station may operate continuously.

Power is fed from the transmitter to a helix house at the base of each array through an underground coaxial transmission system. The helix house contains a tuning unit for the array and provides six feed points on its roof for feeding six vertical "up-leads" which are the radiating elements of the array. The "up-leads" are equally spaced on a circle of diameter 600 ft., providing a large effective diameter for improved bandwidth.

A large buried radial-wire ground system helps to provide a low-loss ground return for the antenna currents. The station is located on a peninsula, and the ground system is terminated in the ocean by means of sea anchors which extend about 200 ft. into the ocean.

The principal characteristics of the antenna are:

Operating Frequency	14 Kc/s
Relative Height H/λ	0.0139
Radiation Resistance	0.08 ohm
Input Resistance	0.16 ohm (dual) 0.24 ohm (single)
Radiation Efficiency	0.50 (dual) 0.33 (single)
Max. Antenna Current	3500 A (dual) 2500 A (single)
Relative Bandwidth	0.37% (dual) 0.27% (single)
Bandwidth	51 cps (dual) 39 cps (single)
Max. Rated Power	2000 Kw (dual) 1000 Kw (single)

The Forestport Antenna consists of one 1205-ft. base insulated guyed tower. The six top guy wires are utilized to provide top-loading and to make the antenna self-resonant at 100 Kc/s . The principal antenna characteristics are:

Operating Frequency	10.2 Kc/s
Relative height H/λ	0.0125
Radiation Resistance	0.071 ohm
Maximum Antenna Current	85 A
Maximum Radiated Power	500 watts

The Jim Creek Antenna (Arlington, Washington) utilizes a long, tapered valley between two mountains (Blue Mt. and Wheeler Mt.); twelve towers, each 200-ft high, are arranged on the crests of the mountains, and support ten spans, of lengths varying between 8500 ft. and 5000 ft. (Fig.6). The spans consist of 1.01-in. cable made of 37 strands of No. 7 hard-drawn copper wire; they can be separated into two sections. The sags vary with the length of each span, and are 1000 feet for the longest span and 500 feet for the shortest. Downleads from each span, consisting of 0.92-in. hollow copper tubing, are held in tension and connected at the base to horizontal feeds which run along the foot of each mountain and are supported by 125-ft. towers. These feeds are connected, each to half of the transmitter.

The total area covered by the antenna is 435 acres , and the area between the twelve support towers is 725 acres .

The principal characteristics of the Jim Creek Antenna are:

Operation Frequency	15.3 Kc/s
Relative Height H/λ	
Radiation Resistance	0.073 ohm
Input Resistance	0.340 ohm
Radiation Efficiency	0.21
Max. Antenna Current	2100 A
Relative Bandwidth	0.36%
Bandwidth	55 cps
Max. Rated Power	320 Kw

The Annapolis Antenna installation consists of nine 600-ft. towers arranged over an extension of 4300 feet , as shown in Fig. 7; the separation between opposite towers is 850 ft. , and the separation between adjacent towers is 1000 ft. The towers are connected with transversal and with longitudinal spans, with sags of the order of 130 ft . Downleads are connected to the mid-points of two spans and to tuning coils; one downlead only is connected to the transmitter. The ground system extends only to the area under the antenna, and consists of wires buried 10-ft. deep and spaced 20-ft. apart.

The principal characteristics of the Annapolis Antenna system are:

Operation Frequency	18 Kc/s
Relative Height H/λ	0.011
Radiation Resistance	0.045 ohms
Input Resistance	0.265 ohms
Radiation Efficiency	0.17
Max. Antenna Current	1578 A
Relative Bandwidth	0.16
Bandwidth	10 cps
Max. Rated Power	322 Kw

The Lualualei Antenna installation (Oahu, Hawaii) consists of seven 600-ft. towers arranged in a geometry similar to that of the Annapolis Antenna; the spacing between opposite towers is 1000 ft. and that between adjacent towers is 1250 ft . Transversal and longitudinal spans, with sags

of the order of 160 ft., are used. The conductors are hollow copper cables 1" or 0.8" in diameter. Downleads are connected to two of the spans, and include tuning coils; one downlead goes to ground, and the other one is connected to the transmitter.

The principal characteristics of the Lualualei Antenna are:

Operating Frequency	15 Kc/s
Relative Height H/λ	0.012
Radiation Resistance	0.045 ohm
Input Resistance	0.200 ohm
Radiation Efficiency	0.22
Max. Antenna Current	988 A
Relative Bandwidth	0.08%
Bandwidth	12 cps
Max. Rated Power	44 Kw

The Rocky Point Antenna installation (L.I., N.Y.) consists of two sections, each having six 400-ft. towers arranged as shown in Fig. 8, with spacing between towers of the order of 1250 ft., and with transversal dimension of the order of 150 ft. The inside four towers are connected to downleads and to suitable tuning coils. The ground plane consists of numerous wires (for a total length of 200 mi.), buried at a depth of 18" in the ground. The principal characteristics of the Rocky Point Antenna are:

Operating Frequency	15.789 Kc/s
Relative Height H/λ	0.0063
Radiation Resistance	0.03
Input Resistance	0.40
Radiation Efficiency	0.07
Max. Antenna Current	670 A
Relative Bandwidth	0.2%
Max. Rated Power	13.4 Kw

The Rugby Antenna installation (England) consists of two sections, each built around one 820-ft. tower; these two towers are 1320-ft. apart, and are fed from the same transmitter, which is located at the half-way point. The top loads of the two sections are supported respectively by eight and by six towers arranged symmetrically around each center tower (Fig. 9). The

total area covered by the antennas is one-and-a-half miles long by one mile wide. The ground system consists of wires which follow the shape of the top load and are spaced 40-ft. to 80-ft.; the larger section has a buried ground plane, and the smaller section has a counterpoise about 16-ft. above ground (Fig. 10).

The principal characteristics of the antenna are:

Operating Frequency	16 Kc/s
Relative Height H/λ	0.0134
Radiation Resistance	0.1 ohm
Input Resistance	0.47 ohm
Radiation Efficiency	0.21
Max. Antenna Current	720 A
Relative Bandwidth	0.28%
Bandwidth	45 cps
Max. Rated Power	52 Kw

The Haiku Antenna (Hawaii) is similar to the Jim Creek installation, except that it is supported between two mountain tops, without towers; four spans, each 4500-ft. long and with downleads 1450-ft. high, are used.

The principal antenna characteristics are:

Operating Frequency	10.68 Kc/s
Relative Height H/λ	
Radiation Resistance	0.31 ohm
Input Resistance	0.86 ohm
Radiation Efficiency	0.36
Max. Antenna Current	325 A
Relative Bandwidth	0.3%
Bandwidth	51.5 cps
Max. Rated Power	330 Kw

The New Brunswick Antenna (N.J.) is similar to the Rocky Point installation, and consists of a number of 400-ft-high towers arranged in pairs on opposite sides of a parallel 600-ft.-wide strip and on a length of 5000 feet. Downleads are connected to the mid-point of each span (Fig. 11). The ground plane consists of a large number of wires buried at 18-in. depth and parallel to the overhead wires.

The principal characteristics of the New Brunswick Antenna are:

Operating Frequency	22.14 Kc/s
Relative Height H/ λ	0.0089
Radiation Resistance	0.039 ohm
Input Resistance	0.35 ohm
Radiation Efficiency	0.11
Max. Antenna Current	615 A
Relative Bandwidth	0.2%
Bandwidth	44 cps
Max. Rated Power	14.8 Kw

The Canal Zone Antenna installation is similar to that of Annapolis, except that it has a larger ground-plane area. The principal characteristics are:

Operating Frequency	15.5 Kc/s
Relative Height H/ λ	0.0095
Radiation Resistance	0.048 ohm
Input Resistance	0.48 ohm
Radiation Efficiency	0.10
Max. Antenna Current	675 A
Relative Bandwidth	0.14%
Bandwidth	23 cps
Max. Rated Power	18 Kw

The Marion Antenna installation (Massachusetts) is similar to that of New Brunswick, N.J. The principal characteristics are:

Operating Frequency	11.55 Kc/s
Relative Height H/ λ	0.0047
Radiation Resistance	0.051 ohm
Input Resistance	0.40 ohm
Radiation Efficiency	0.14
Max. Antenna Current	600 A
Relative Bandwidth	0.39%
Bandwidth	45 cps
Max. Rated Power	18.3 Kw

The Tuckerton Antenna installation (N.J.) uses a center tower 780-ft. high, and a top load of umbrella type, of diameter 3200 ft., sustained by 300-ft. peripheral towers (Fig. 12). The principal characteristics of the antenna are:

Operating Frequency	18 Kc/s
Relative Height H/λ	0.0143
Radiation Resistance	0.052 ohm
Input Resistance	0.24 ohm
Radiation Efficiency	0.21
Max. Antenna Current	913 A
Relative Bandwidth	0.13%
Bandwidth	24 cps
Max. Rated Power	43 Kw

In order to obtain a basis for the comparison of the characteristics of various antennas, the values of radiation resistance, relative bandwidth, product of efficiency times relative bandwidth, maximum power radiated have been tabulated as functions of the relative height H/λ ; it should be noted that some of the data used may be approximate or obsolete.

TABLE III

SUMMARY OF VLF ANTENNA CHARACTERISTICS

	H/λ	R_{rad}	BW/f%	η BW/f%	P_{max}(Kw)
Cutler (dual)	0.0139	0.08	0.37	0.185	2000
Cutler (single)	0.0139	0.08	0.27	0.09	1000
Forestport	0.0125	0.071	-	-	0.5(rad.)
Jim Creek	-	0.073	0.36	0.075	320
Annapolis	0.011	0.045	0.1	0.017	322
Lualualei	0.012	0.045	0.08	0.0175	44
Rocky Point	0.0063	0.03	0.2	0.021	13.4
Rugby	0.0134	0.1	0.28	0.059	52
Haiku	-	0.31	0.3	0.093	330
New Brunswick	0.0069	0.039	0.2	0.022	14.8
Canal Zone	0.0095	0.048	0.14	0.014	18
Marion	0.0047	0.051	0.39	0.055	18.3
Tuckerton	0.0143	0.052	0.13	0.0272	43

The values of Table III have been computed on the basis of data taken mainly from the following sources:

a) ITTFL Trip Report on visit to Cutler, Maine, on 8-20-63

b) California Institute Technical Report No. 4 - A New Transmitting Antenna System for VLF - by W. VonTuyl Rusch - June 1959

c) Illinois Institute Technical Report - RFD Antenna Technique Survey - Sept. 1961

d) Deco Electr. Report No. 42-F - Forestport Antenna Study - January 1962

Of the various quantities listed in Table III, only the radiation resistance may be related directly to the relative geometric height H/λ ; a detailed discussion of such relationship is given in the following Section. The relative bandwidth is a function of the quality factor Q characteristic of the antenna input impedance function; therefore, it depends mainly upon the ratio of the input reactance to the input resistance--i.e., upon the antenna effective diameter and upon the loss resistance. The product of the radiation efficiency times the relative bandwidth is approximately independent of the loss resistance and, therefore, represents a quality factor of the antenna design; within certain limitations, it is possible to trade efficiency for relative bandwidth.

5. RADIATION RESISTANCE OF VLF ANTENNAS

The radiation resistance of VLF antennas may be computed approximately by means of the relationship:

$$R_{rad} = 1600 \left(\frac{H}{\lambda}\right)^2 \left[\frac{b/H}{1+b/H} + \frac{1}{4}\,\frac{1}{(1+b/H)^2}\right] \qquad (43)$$

In this expression, b is the additional vertical length that is equivalent to the top load--i.e., that would provide the same current distribution (Fig. 13); a plot of Equation 43 as a function of H/λ for various values of the parameter b/H is given in Fig. 14. In this figure, there are also shown data taken from Table III; most of these appear to cluster about the curve corresponding to zero top-loading.

In the case of ferrite-loaded antennas, an accurate expression of the radiation resistance is not available. The experimental results of HF antenna without top load which have been reported in Table III have been used to compute $R_r = \eta R_{in}$; these values have been plotted versus H/λ_o in Fig. 15, along with the curve representing Equa. 43 for $b/H = 0$. It is seen that the values of R_r are approximately 2 to 5 times larger than those given by the latter curve. In the graphs of Fig. 14 and of Fig. 15 is shown the value of radiation resistance measured with a LF ferrite-loaded and top-loaded antenna (81.7Kc), which is described in a following Section; this value is $f = 81.7$Kc , $H/\lambda_o = 0.008$, $R_r = 0.1$ ohm.

6. DESIGN OF THE GROUND PLANE

The design of the ground plane is important in determining the final radiation efficiency of the antenna. Analytical investigations of this problem, leading to a study of the effect of radial-wire diameter and length on the antenna input impedance and on the field propagation, have been made recently*. In particular, with reference to a radial ground, Abbott has computed the optimum number of radials, their optimum length, and the power dissipated in the ground as functions of the frequency of operation f , of the conductivity σ , of the soil permeability μ , of the annual copper cost, and of the annual cost of the power dissipated in the ground.

---

* F. R. Abbott - Design of Optimum Buried-Conductor RF Ground - Proc. IRE, July 1952, pp 846-852.

J. R. West and W. A. Pope - The Characteristics of a Vertical Antenna with a Radial Conductor Ground System - Appl. Science Res. B, (1954) Vol. 4 - pp. 177-195.

J. R. West and W. A. Pope - Input Resistance of L.F. Unipole Aerials - Wireless Eng., (May 1955) Vol. 32 - pp. 131-138.

S. W. Maley and R. J. King - Impedance of a Monopole Antenna with a Radial Wire Ground System on an Imperfectly Conducting Half-Space - J. Res. NBS 66 D, (1962) No. 2 - pp. 175-180; and J. Res. NBS 68D , (1964) pp. 157-163.

Assuming a spacing between wires d and a power dissipated per $m^2 w$, the total annual cost is expressed as:

$$K_t = K_{1/d} + K_2 w \tag{44}$$

where

$$K_2 = (C_a + C_b)\, W \tag{45}$$

and C_a = annual amortization cost of the station exclusive of the ground system, C_b = annual operating cost of the station, W = average input power to the antenna.

The loss per unit surface w is expressed as follows:

$$w = |J^2|d^2 \sqrt{\frac{\sigma f^3 \mu^3}{4\pi}} \log_e^2 \frac{d}{2\pi a} = C_1 d^2/K_2 \tag{46}$$

where

$$C_1 = K_2 \left(|J^2| \frac{\sigma f^3 \mu^3}{4\pi} \log_e^2 \frac{d}{2\pi a} \right) \tag{48}$$

There follows:

$K_t = C_1 d^2 + K_1/d$ dollars per year. This cost is minimum when the following identity is satisfied:

$$d^3 \log_{10}^2 \frac{d}{2\pi a} = \frac{2.38 \times 10^8 \times K}{K_2 \, |J^2| \sqrt{\sigma f^3}} = F_1 \tag{49}$$

The surface current density $|J|$ is obtained from the equation:

$$\frac{\lambda |J|}{I_o} = \frac{1}{2\pi \frac{r}{\lambda} \sin\beta h} \left(\epsilon^{-j\beta\rho} - \epsilon^{-j\beta\rho} \cos\beta h\right) \tag{50}$$

where

ρ and r are respectively the distances from the top and from the base of the antenna

I_o is the antenna base current

The quantity given by Equation 50 is plotted in Fig. 16 as a function of r/λ, using as a parameter h/λ.

For given values of J, σ, f, K_1/K_2, one can compute the quantity F_1 of Equation 49 and can derive the optimum spacing d.

The number of radials is computed with the relation:

$$N = 2\pi r/d \tag{51}$$

The optimum length of the radials may be computed on the basis of the value for which the distance between wires makes the power dissipated per unit surface practically independent of the presence of the wires. This is obtained approximately when the following identity is satisfied:

$$F_2 = d_t \log_{10}^2\left(\frac{d_t}{2\pi a}\right) = \frac{1.88 \times 10^6}{f\sigma} \tag{52}$$

where d_t is the terminal distance. From the value d_t, the radial length r_t follows:

$$r_t = Nd_t/2\pi \tag{53}$$

Finally, the total power absorbed in the soil may be computed with the integral:

$$P = \int_0^{2\pi}\int_{r_1}^{r_t} w \, r dr d\varphi \tag{54}$$

The effective antenna base impedance depends upon the radiation resistance, ground plane losses, the corona and insulator losses, etc. If the latter can be neglected, the antenna impedance may be expressed as follows:

$$Z_{in} = Z^{\infty} + \frac{2\pi}{I_o^2} \int_{r_o}^{r_t} \eta_c(r) \left[H_{\phi}(r,o) \right]^2 r dr \; + \qquad (55)$$

$$\frac{2\pi}{I_o^2} \int_{r_t}^{\infty} \eta_g \left[H_{\phi}^{\infty}(r,o) \right]^2 r dr$$

where

Z^{∞} is the monopole base impedance obtained in the case of a perfectly conducting ground

r_o and r_t are respectively the radii of the counter-weight and of the radial ground plane (Fig. 17)

H_{ϕ} (r,o) is the tangential component of the magnetic field for the case of a perfectly conducting ground

η_c is the effective surface impedance of the ground plane

i.e.,

$$\eta_c = \frac{\eta_g \; \eta_w}{\eta_g + \eta_w} \qquad (56)$$

where

$$\eta_w = \frac{j2\pi\eta_o \; r}{\lambda \; N} \; \ell n \frac{r}{Na}$$

$$\eta_o = \sqrt{\mu_o/\epsilon_o} \; , \quad \eta_g = \left[\frac{j\omega\mu}{\sigma + j\omega\epsilon} \right]^{1/2} \qquad (57)$$

The tangential component of the magnetic field may be computed approximately with the expression:

$$H_{\varphi}^{\infty}(r,o) = \frac{jI_o}{2\pi \sin\alpha} \left[\frac{\epsilon^{-j\beta\rho}}{r} \cos(\beta h-\alpha) - \frac{\epsilon^{-j\beta r}}{r} \cos\alpha + \right.$$

$$\left. \frac{jh\epsilon^{-j\beta\rho}}{r\rho} \sin(\beta h-\alpha) \right] \qquad (58)$$

where

$\alpha = \beta(h+h')$

h is the actual monopole height

h' is the additional height equivalent to the top-loading

$\rho = (r^2+h^2)^{1/2}$

The relation (Equation 58) represents a good approximation in the case of symmetric top-loading.

The impedance contribution due to the ground plane losses may be expressed with the relationship:

$$\Delta Z = Z - Z = \Delta R + j\Delta X \tag{59}$$

where the right-hand side is obtained from Equation 55.

It is of interest to show practical examples of design of ground plane based on the above-discussed theories.

Assume that the buried wire has diameter 3 mm (Copper No. 8 AWG, with a = 0.00325 m) . One can readily compute the quantities F_1 and F_2 of Equations 49 and 52 respectively; i.e.,

$$F_1 = d^3\log_{10}\left(\frac{d}{2\pi a}\right), \qquad F_2 = d_t\log_{10}^2\left(\frac{d_t}{2\pi a}\right) \tag{60}$$

as functions of d (or d_t) ; such plots are shown in Fig. 18.

Assume operation at a frequency f = 600 Kc/s, with a quarter-wave monopole, having radiation resistance 40 ohm , antenna base current 5A , radiated power 1 Kw . Let:

$$K_1 = 0.01 \text{ dollar}, \quad K_2 = 1$$

where K_1 is the cost of amortization of one meter of buried No. 8 copper wire

K_2 is the cost per year of one watt of RF power

Assume that the ground conductivity is $\sigma = 2 \times 10^{-3}$ mho/m. From Equation 52, one finds $F_2 = 1.566 \times 10^3$ and $d_t = 12.5$ m ; entering the latter

value into Equation 49 or Fig. 18, one finds the value of $F_1 = 1.86 \times 10^4$ and computes that of $|J| = 2.48 \times 10^{-3}$ A/m. Finally, computing the quantity $|J| \lambda/I_o = 0.248$, and using the graph of Fig. 16, one finds the value of $r_t/\lambda = 0.64$ (i.e., $r_t = 320$ m). Finally, the number of radials is obtained using Equation 53; i.e.,

$$N = 2\pi\, r_t/d_t = 161 \tag{61}$$

In order to compute now the actual increment of input impedance of the monopole antenna due to the ground plane, one makes use of Equations 55, 58, and 59. For the present example, assuming that ϵ_r for the ground is 10 , one has:

$$\begin{aligned} &\alpha = \beta h = \pi/2\,, \quad a/\lambda = 3 \times 10^{-6}, \\ &\eta_g = \sqrt{j}\ 48.5 \times \epsilon^{-j\,0.166}\ \text{ohm}\,, \quad h/\lambda = 0.25,\ r_t/\lambda = 0.64\,, \\ &N = 161 \end{aligned} \tag{62}$$

There follows:

$$\Delta R \cong 1.1\,, \quad \Delta X \cong 0.1$$

A graphical representation of the variation of ΔR and of ΔX as a function of r_t/λ (assuming $h/\lambda = 0.25$, $a/\lambda = 10^{-6}$, $\alpha = \pi/2$, $\eta_g = \sqrt{j}\ 37.7$, and taking as a parameter the number N) is shown in Fig. 19.

More generally, the results of the computations of ΔR and of ΔX as a function of r_t/λ and with parameter N are shown in Fig. 20 a) and b) for the cases $h/\lambda = 0.1$, $h/\lambda = 0.01$, respectively, assuming again $a/\lambda = 10^{-6}$, $\alpha = \pi/2$, and $\eta_g = \sqrt{j}\ 37.7$.

It is of interest to note that the increase ΔR with diminishing radial length r_t/λ occurs at a greater rate in the case of short dipoles than in that of quarter-wave dipoles.

The effect of the variation of the size of the buried wire is generally small. In Fig. 21 is shown the result of the computation of ΔR and ΔX versus r_t/λ for a quarter-wave dipole, assuming $N = 100$, $\eta_g = \sqrt{j}\,11$, and taking as a parameter a/λ; in Fig. 22 is shown the result of the computation of ΔR and ΔX versus a/λ for various values of r_t/λ and for the case $h/\lambda = 0.05$, $N = 100$, $\alpha = \pi/2$, $\eta_g = \sqrt{j}\,37.7$. It is seen that the input impedance of the antenna is a very slowly varying function of a/λ for the cases studied.

The effect of the top-loading parameter α is shown in Fig. 23 for the case $N = 100$, $a/\lambda = 10^{-6}$, $\eta_g = \sqrt{j}\,37.7$, and $h/\lambda = 0.01$, 0.05, & 0.1 respectively. As the top-loading is increased, ΔR is also increased because larger currents are passed through the ground; in addition, the effect of the top-loading is greater the greater the relative height of the antenna.

In comparing the effects of top-loading and of electrical length on the value of ΔR, it is of interest to take into account simultaneously also the value of the radiation resistance. For short monopoles with and without top-loading, the latter may be computed approximately with the relationship:

$$
\begin{aligned}
R_r &\cong 160\,\pi^2 (h/\lambda)^2 \text{ ohm for } \alpha = \pi/2 \\
R_r &\cong 40\,\pi^2 (h/\lambda)^2 \text{ ohm for } \alpha = 0
\end{aligned}
\qquad (63)
$$

These relationships have been plotted in Fig. 24 a) and b), along with the corresponding graphs showing ΔR versus (h/λ) for $\alpha = \pi/2$ or 0, and for various values of r_t/λ. It is of interest to consider the value of r_t/λ for which $R_r = \Delta R$ (50% efficiency); from Fig. 24, it is seen that, in the case of top-loaded monopoles, the latter value is smaller, the smaller h/λ.

Finally, the effect of variations of the ground-surface impedance is illustrated in Fig. 25 for the case $N = 100$, $\alpha = \pi/2$, $a/\lambda = 10^{-6}$, $h/\lambda = 0.1$, and $\delta = |\eta_g|/\eta_o = \left(\frac{\omega\epsilon_o}{\sigma}\right)^{1/2} = 0.003$ to 0.2. It is seen that

the incremental resistance increases approximately in direct proportion to $\sqrt{f/\sigma}$. These results illustrate the importance of building the antenna on a ground having good conductivity σ ; the relationship between δ and σ is illustrated in Fig. 26 for various frequency values.

Recapitulating, the design of the ground plane may be conducted with fair accuracy using the relationships and graphs given previously. In particular, one can determine the optimum number N and the optimum radial length for given values of h/λ, a/λ, α and δ; in most cases, it is found that $N \cong 250$ and $r_t/\lambda \cong 0.2$ are convenient values.

7. DESIGN OF TOP LOAD

The effect of top-loading the antenna is beneficial in general since it reduces the size of the input inductor required to tune the base input impedance and lowers the operating voltage of the radiator. This results in a decrease of the losses due to the resistance of the input inductor, to the corona effects, to the insulator's surface resistance, etc. It is of interest to investigate the effect of the top-load on the ground losses.

Wait* has shown that the earth currents are not modified significantly by the presence of a symmetrical top-loading. On the other hand, Knudsen** has shown that, when the top-loading is unsymmetrical as in the case of L- or T- type structures, a circumferential component of the ground current arises which may contribute considerably to the ground losses because it is perpendicular to the radial ground wires.

Assume that the antenna current distribution is linear (Fig. 27); i.e.,

$$I(Z) = I_o \left(1 - \frac{Z}{h+h'}\right) \tag{6?}$$

where I_o is the base current; in first approximation, it is found that the normalized contribution to the earth current density distribution due to the vertical member of the antenna is radial and is expressed as follows:

---

* J. R. Wait - Earth Currents Near a Monopole Antenna with Symmetrical Top-Loading - J. Res. NBS, Vol. 62 (June 1959).

** H. L. Knudsen - Earth Currents Near a Top-Loaded Monopole Antenna with Special Regard to Electrically Small L- and T-Antennas - J. Res. NBS, Vol. 62 (June 1959).

$$J_\rho^{\,v} = -\frac{\epsilon^{jk\rho}}{2\pi} \; \frac{1}{\frac{\rho}{h}\; 1+(\frac{\rho}{h})^2} - jkh \tan^{-1}\left(\frac{h}{\rho}\right) \; \frac{1+2h'/h}{2\,(1+h/h')} \tag{65}$$

where h' is the additional height component equivalent to the top-loading. Assuming that h/λ is very small ($\frac{h}{\lambda} = 0$ and $\frac{h}{\lambda} = 0.06$), the above quantity varies with distance ρ/h as shown in Fig. 28, where parameter h'/h has been used.

The contribution of the horizontal top-load wires is found to be parallel to the wires; considering a single wire at azimuth β, and assuming that h/λ is negligible, the normalized surface current density $J_s^{\,h}$ at the ground plane at azimuth $\phi = \beta$ and $\phi = \beta + \pi$ varies as shown in Fig. 29 as a function of ρ/h with parameter h'/h; similarly, in Fig. 30, the corresponding case for $h/\lambda = 0.06$ is given. This result illustrates the effect of an L-type top-loading (Fig. 31). The radial and azimuthal components of J^h are computed with the relations:

$$\begin{aligned} J_\rho^{\,h} &= J_s^{\,h} \cos(\phi-\beta) \\ J_\phi^{\,h} &= J_s^{\,h} \sin(\phi-\beta) \end{aligned} \tag{66}$$

Considering the ratio $J_\rho^{\,h}/J_\rho^{\,v}$, it is seen that this is very small; however, the presence of $J_\varphi^{\,h}$ indicates that losses occur in the ground if the buried system of wires is radial. The ratio $J_\varphi^{\,h}/J_\rho^{\,v}$ has been plotted in Fig. 32 a) and b) for the cases $h/\lambda = 0$; and a) $\phi - \beta = 45°$, b) $\phi - \beta = 135°$. The latter quotient is zero in correspondence of $\phi - \beta = 0$ and $\phi - \beta = 180°$.

Consider now the case of a T-type antenna (Fig. 31 b)), for which the horizontal top-loading is symmetrical, using the results for the L-type antenna. The contribution to the radial component of the surface current density is still small and of the same order of magnitude of that of the L antenna; on the other hand, the circumferential component of the surface

current density is very low as it is seen from the graph of Fig. 33, which gives the ratio $j_{\varphi}^{h}/J_{\rho}^{v}$ for the case $h/\lambda = 0$ and $\phi - \beta = 45°$.

In conclusion, it appears that the losses in a radial-type ground plane are increased when the top-loading is not symmetrical. These losses could be reduced by the addition of circumferential buried wires; however, if closed loops are formed in the ground, these could give rise to circulating currents and produce additional losses.

8. EXPERIMENTAL VERIFICATION OF LOW-FREQUENCY FERRITE ANTENNA DESIGN

Various experimental verifications of the operation of ferrite-loaded radiators at low frequencies have been conducted in connection with the present investigation; these were aimed at determining the actual wavelength reduction provided by means of ferrite loading, the effect of various types of top-loading, and the effect of various folding techniques.

In addition, under the same contract NOnr 3358, a design of ferrite-loaded transportable-type radiator has been conducted, the results of which provide invaluable data on the properties of practical ferrite-loaded antennas. The latter work (which, at the time of this writing, was still under development) is discussed in a separate Report entitled: "Feasibility of Design of a Transportable L.F. High-Power Ferrite-Loaded Radiator". In the following, a number of basic results are presented together with a discussion of their significance in connection with the proposed design of an Omega ferrite-loaded antenna.

The dimensions of the ferrite radiator used in the preliminary design of the Omega antenna were I.D. = 0.75", O.D. = 3" ; using the theoretical analysis of Section 2 and the graphical solution of Fig. 3, one finds that, at 10.2 Kc/s , the wavelength shortening ratio is $\lambda_z/\lambda_o = 0.27$. A practical verification of the properties of such type of loading has been made constructing radiator elements of length 10, 20, and 100 feet, and studying their resonant properties. The wavelength shortening ratio has been found to vary with the length of the radiator in the manner shown in Fig. 34; in particular, the ratio is in fact less than the theoretical value of 0.27

and approaches it asymptotically for very large length. It is of interest to note that, for a 500-ft radiator, the ratio would be 0.175, and the self-resonance frequency would be 86 Kc .

Knowing the electrical height of the vertical radiator, one can compute the top-load capacitance required for tuning at 10.2 Kc (λ_o = 29400 m); for example, a 500-ft (152 m) radiator has equivalent height 870 m , and requires a capacitor load having equivalent height 6480 m or electrical height $H/\lambda_o = 0.22$. The actual value of the capacitance depends on the reactive properties of the antenna, on its diameter, type of loading, etc.

The construction of a 100-ft ferrite radiator has provided some information in this connection. Without top-load, the radiator resonates at 400 Kc/s and presents a wavelength shortening ratio of 0.165 ; when top-loaded with an umbrella-type wiring having static capacitance $C = 0.0045\mu F$, the self-resonance of the radiator occurs at $f = 79$ Kc/s . A plot of the input resistance and input reactance of the antenna as function of frequency is given in Fig. 35; in the same graph, the corresponding values of H/λ_z and of H/λ_o are shown. Since the actual height of the ferrite radiator is 30.5 m , its equivalent height is 30.5/0.165 = 185 m , and its electrical height is 185/3800 = 0.0487 . The equivalent height of the top-loading is 0.25 - 0.0487 = 0.2013 ; using transmission line equations, it is seen that the short antenna behaves approximately like a transmission line with characteristic impedance $R_o = 10^4$ ohm.

We can also derive by extrapolation the data pertinent to the operation of the same radiator at 10.2 Kc . We shall assume that the ferrite radiator has a height of 500 feet , for which the wavelength shortening ratio is 0.175, and that the input impedance presents the same general behavior as that of Fig. 35. At 10.2 Kc , the wavelength λ_o is 29,400 m , and the equivalent height and the electrical height of the radiator are respectively 870 m and 0.0295 ; there follows that the equivalent electrical height of the top load is 0.2305 , and its capacitive reactance at 10.2 Kc and its capacitance are respectively -295 ohm and $0.052\mu F$.

The radiation resistance of the 100-ft antenna has been computed from field intensity measurements taken at 2 miles ; the radiation pattern

is shown in Fig. 36 and indicates that the radiation resistance is approximately R_r = 0.10 ohm . Using the relationship:

$$R_r = K \left(\frac{H}{\lambda}\right)^2 \tag{67}$$

and substituting the value $H/\lambda_o = 0.00805$, one finds $K = 1560$, which corresponds well with the well-known value $K = 1600$ applicable in the case of fully top-loaded monopole radiators. Extrapolation of this relationship to the case of the Omega antenna provides the following result:

$$R_r = 1600 \left(\frac{152}{29400}\right)^2 = 0.043 \text{ ohm} \tag{68}$$

It should be noted that the input impedance measured in the case of the 100-ft radiator and shown in the graph of Fig. 35 is about 6 ohm; this large value is due to losses, the source of which has not yet been determined, but could be due to the ground plane, to some lossy antenna component, or to the ferrite. A thorough study of the possible cause of the losses is being made at the present time; no basic reason for the existence of such losses, and no obstacle for its removal, is seen. Finally, other important characteristics of the design are the maximum power radiated and the bandwidth; measurements of the maximum radiated power are expected to be performed in the near future. Such power will depend upon the maximum permissible antenna current. Assuming that a base antenna current of 100 A is permissible, as discussed in Section 3 of this Report, a maximum radiated power per monopole of 430 watts is obtained.

The bandwidth of the ferrite radiator depends upon the characteristics of the input impedance and, therefore, its value must be measured after the loss resistance has been reduced to its minimum value. From the graph of Fig. 35, one notes that, with the high loss resistance of 6.4 ohm , the antenna bandwidth is 1100 c/s , which corresponds to a relative bandwidth value of 1.4% ; if it is assumed that the loss resistance is reduced

to a value of 1 ohm, the expected values of bandwidth and relative bandwidth become 180 c/s and 0.23% respectively.

9. CONCLUSIVE REMARKS

Although the investigation of the design of LF ferrite-loaded antennas has not been completed at the time of the writing of this report, a sufficient amount of data has been obtained to provide a great increase of understanding of the behavior of ferrite-loaded radiators and of the feasibility of design of VLF antennas using such type of loading. The characteristics which await further experimental verification are the loss resistance and the maximum power radiated per monopole.

The following conclusions have been gained from the present investigation:

a) A ferrite radiator of height 500 feet, with full capacitive top-loading for operation at 10.2 Kc, is expected to have a radiation resistance of the order of 0.043 ohm.

b) The radiator may be supported directly with a steel tower without recourse to steel ropes, provided suitable insulators (ex. of Teflon) are used. The radiator may be built in sections of 10-ft length, weighing about 160 lbs. each. The weight of the entire 500-ft radiator is 8000 lbs. The elements may be enclosed within suitable fiberglass cylinders, made hermetic to humidity

c) The antenna installation may be made using multiple radiators arranged as a cage-type structure. The distance between radiators depends upon the allowable reactive interaction between elements. The total area of the installation depends upon the design of the top load. A capacitive load of 0.02μF per monopole has been estimated. Using the equation:

$$C = \frac{\pi \epsilon_o L}{\ell n\ 4\ h/d}$$

for the capacitance of an horizontal wire of length L, diameter d, and height h above the ground, one finds the total length required of a wire.

d) A comparison of characteristics of the Omega ferrite antenna with those of the VLF antennas listed in Table III (p. 27) is instructive. The expected value of H/λ_o is 5.17×10^{-3}, and the expected radiation resistance is 0.043 ohm. If it is assumed that the input resistance may be reduced to 1 ohm and the maximum current per monopole may be made 100 amperes; and if it is assumed that a cage structure of nine monopoles is used, one finds:

	H/λ	R_{rad}	BW/f%	$\frac{BW/f\%}{\eta}$	P_{max} (Radiated)
Omega Ferrite Antenna (Single Radiator)	0.005	0.043	0.23(?)	0.009(?)	430 w(?)
Nine-Radiator Cage	0.005	0.043	0.5 (?)	0.02 (?)	34.7 Kw(?)

These values compare very favorably with those of Table III; when account is taken of the construction costs (which are roughly proportional to the third power of the ratio H/λ), the advantages presented by the ferrite antenna design are evident.

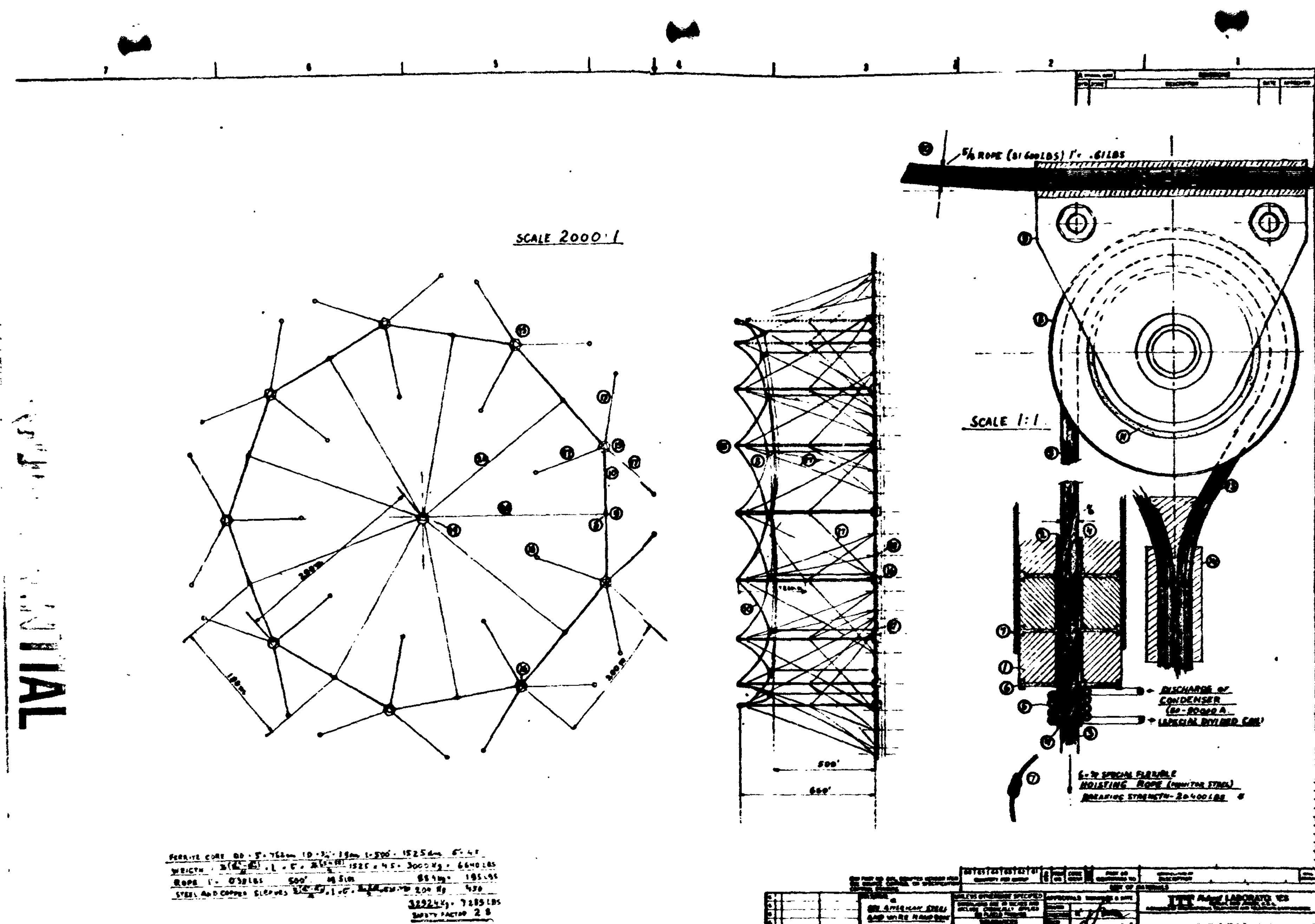

FIG. 1 - PRELIMINARY PROPOSAL OF OMEGA FERRITE ANTENNA

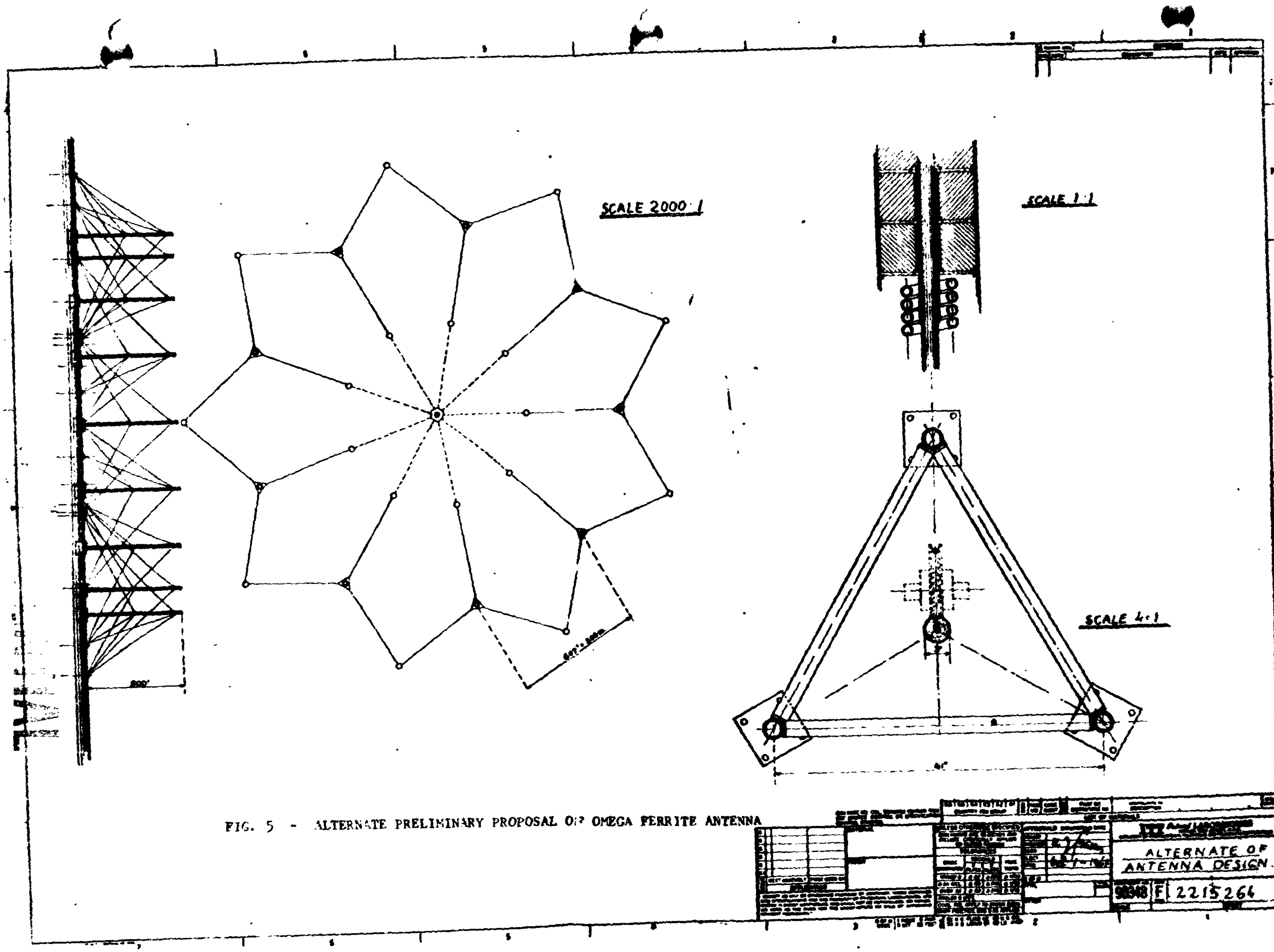

FIG. 5 - ALTERNATE PRELIMINARY PROPOSAL OF OMEGA FERRITE ANTENNA

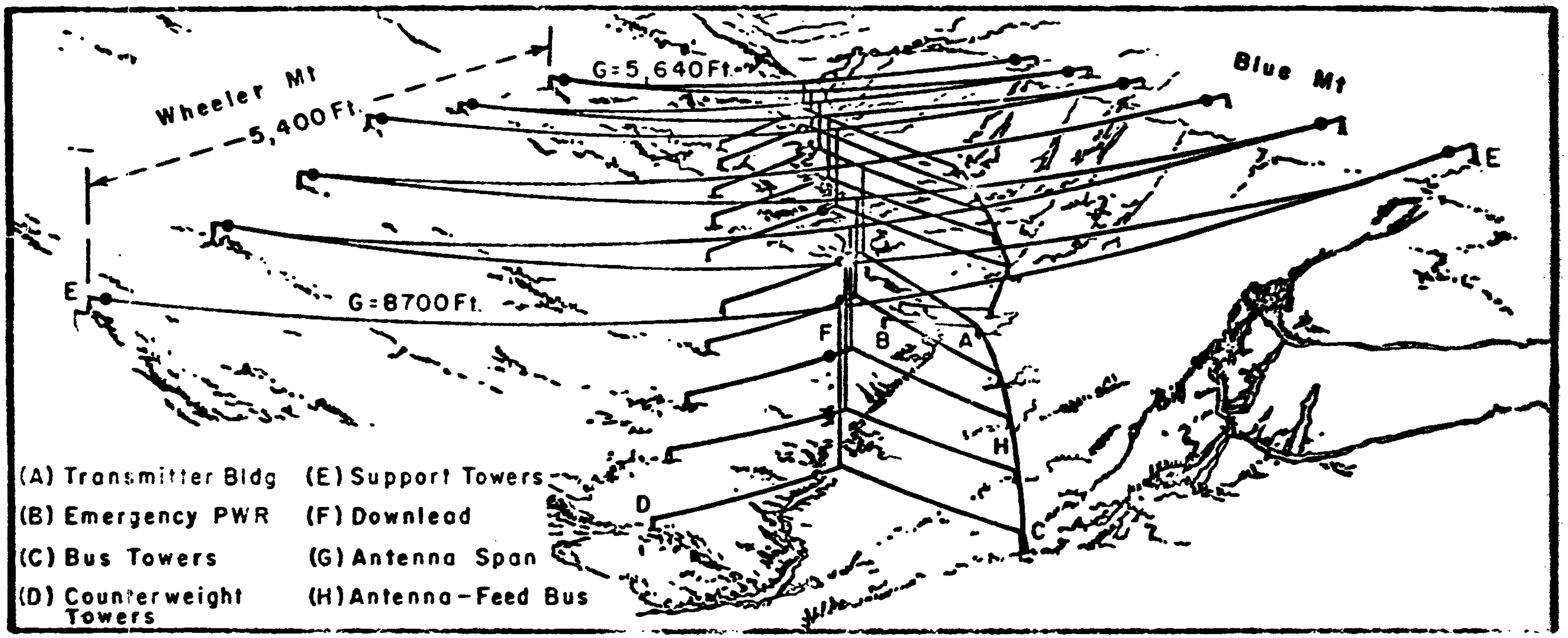

FIGURE 6 - JIM CREEK VLF TRANSMITTING ANTENNA

CONFIDENTIAL

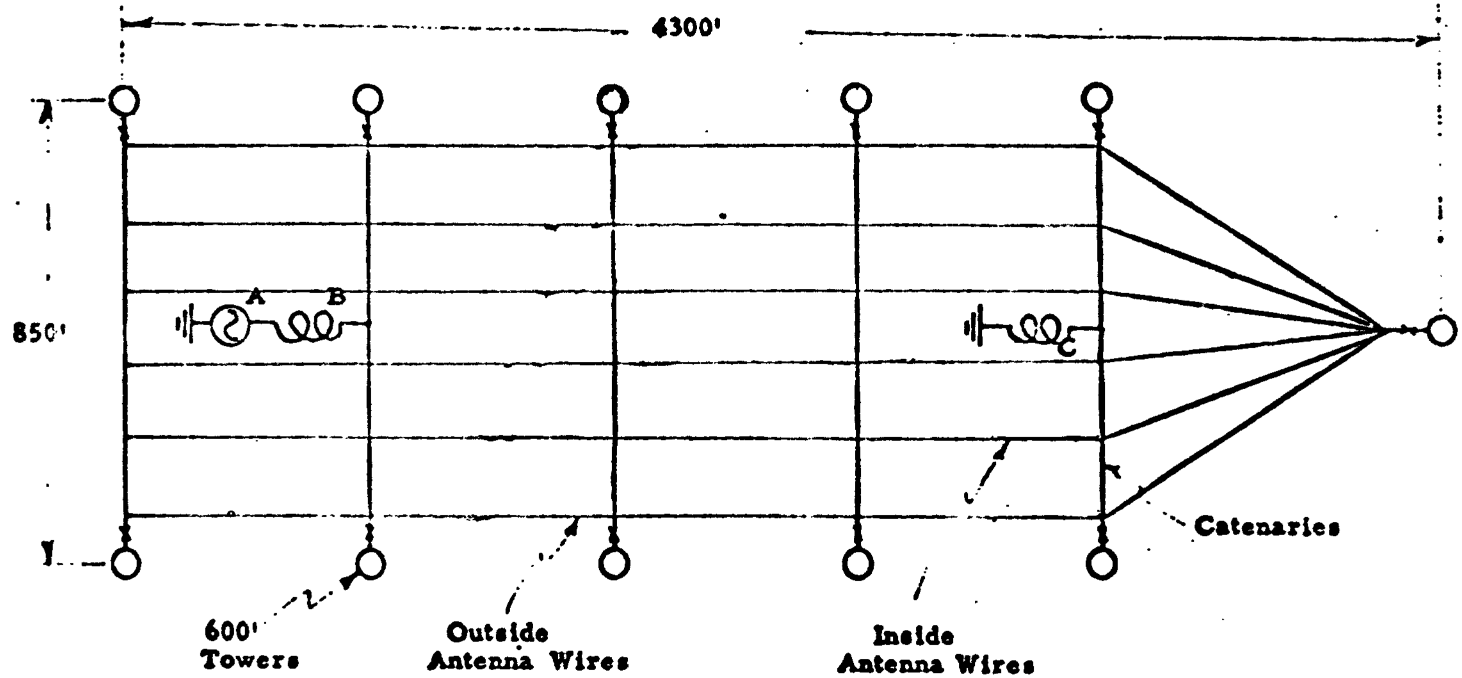

(A) TRANSMITTER
(B) FEED COIL
(C) TUNING COIL

Fig. 7.- DIAGRAM OF THE ANNAPOLIS, MD., ANTENNA

CONFIDENTIAL

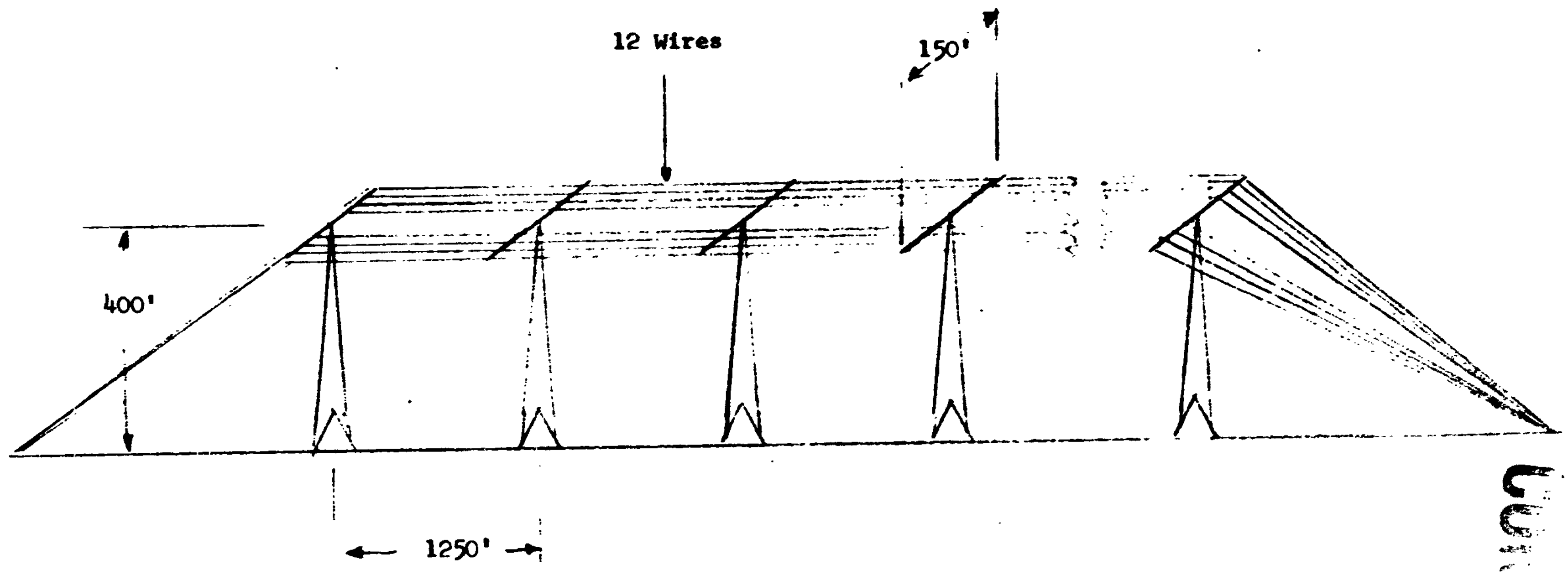

FIG. 8 - ROCKY POINT ANTENNA

CONFIDENTIAL

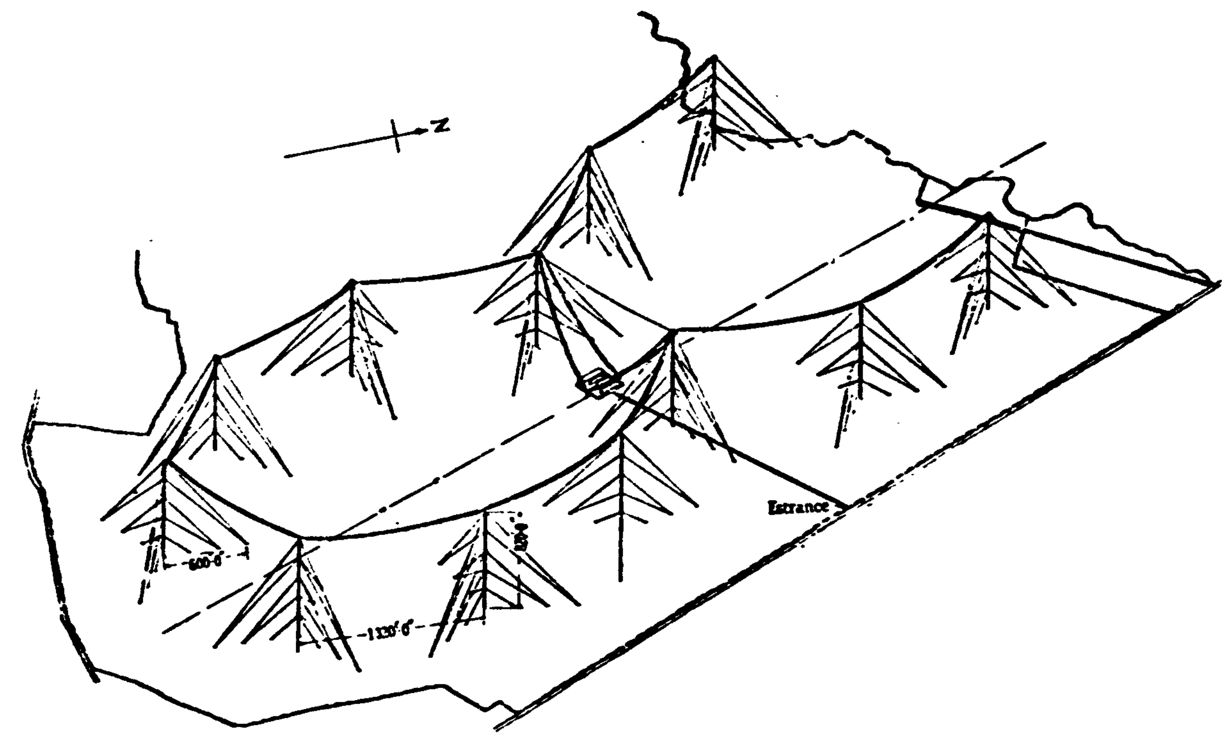

FIGURE 9 - RUGBY GBR TRANSMITTING ANTENNA.

CONFIDENTIAL

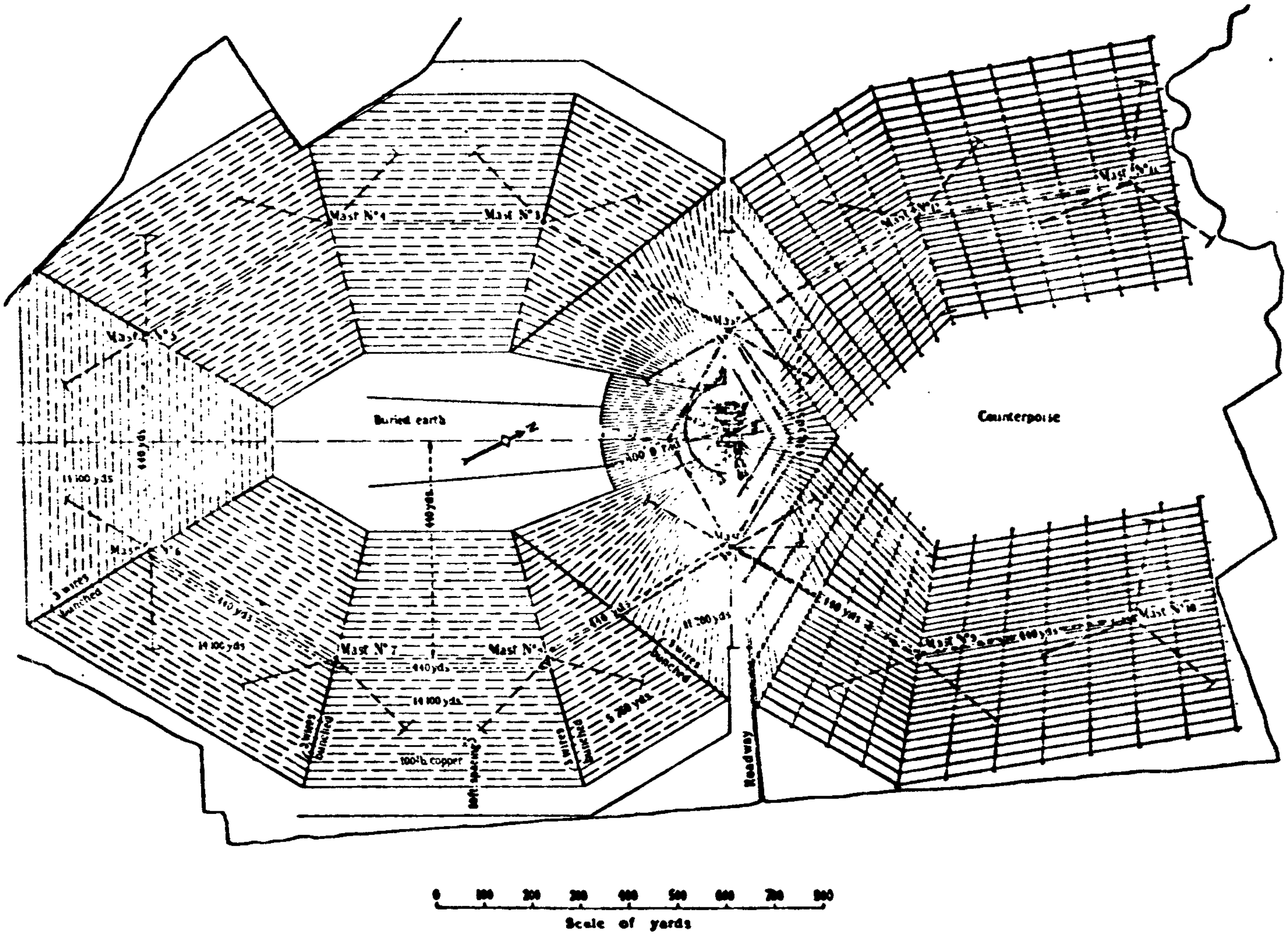

FIGURE 10 - RUGBY GBR TRANSMITTING ANTENNA GROUND SYSTEM.

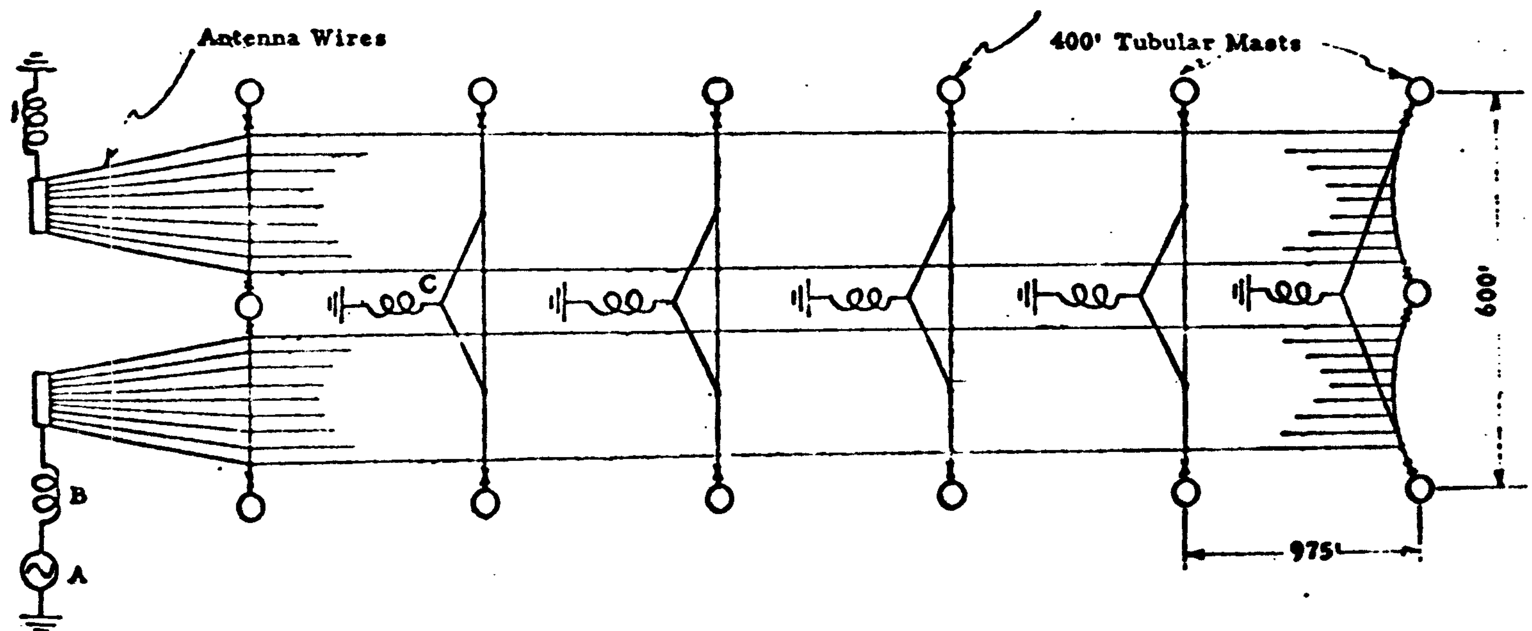

Fig 11-DIAGRAM OF THE MARION, MASS. AND NEW BRUNSWICK, N. J. VLF TRANSMITTING ANTENNAS

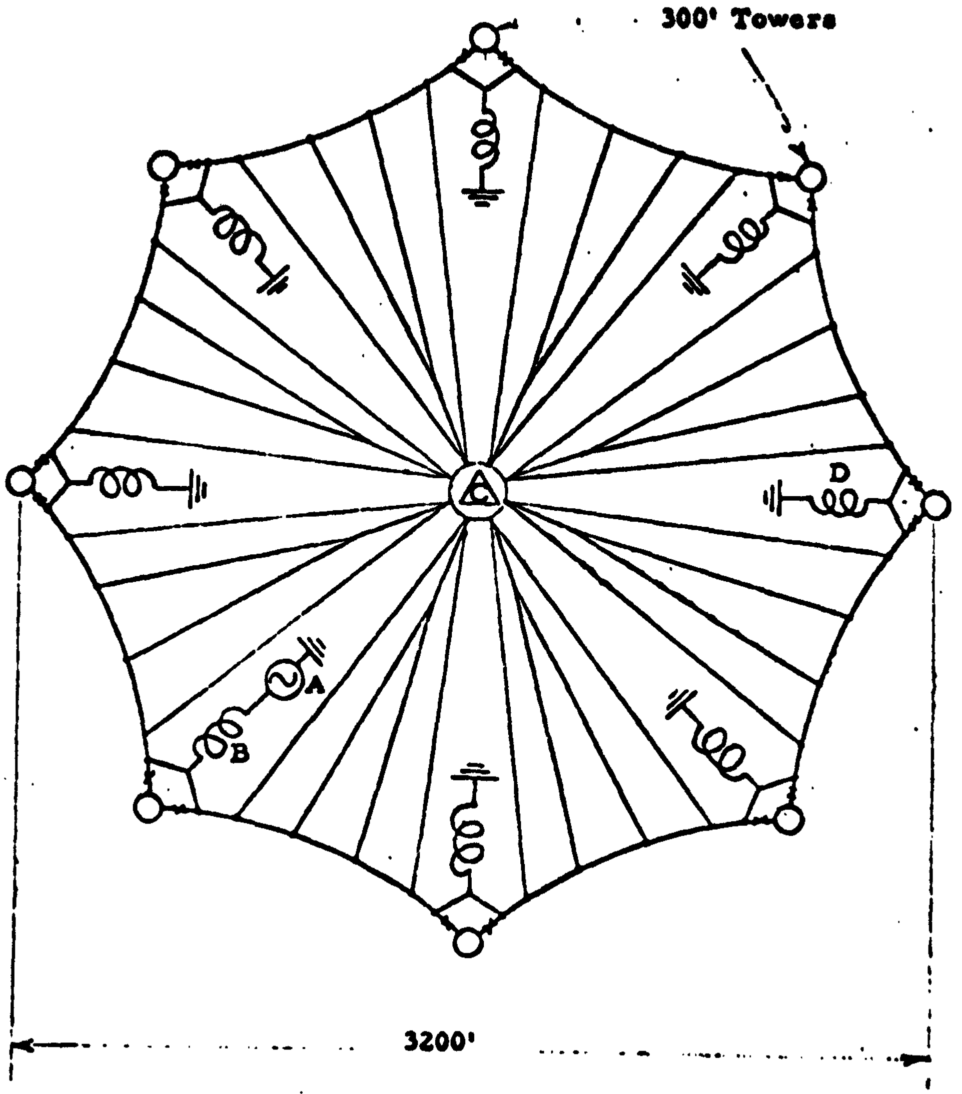

Fig. 12 - DIAGRAM OF THE VLF ANTENNA AT TUCKERTON, N. J.

CONFIDENTIAL

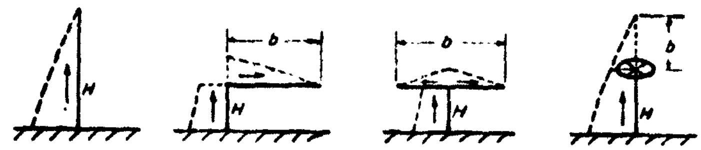

FIG. 13 - EXAMPLES OF TOP-LOADED ANTENNAS

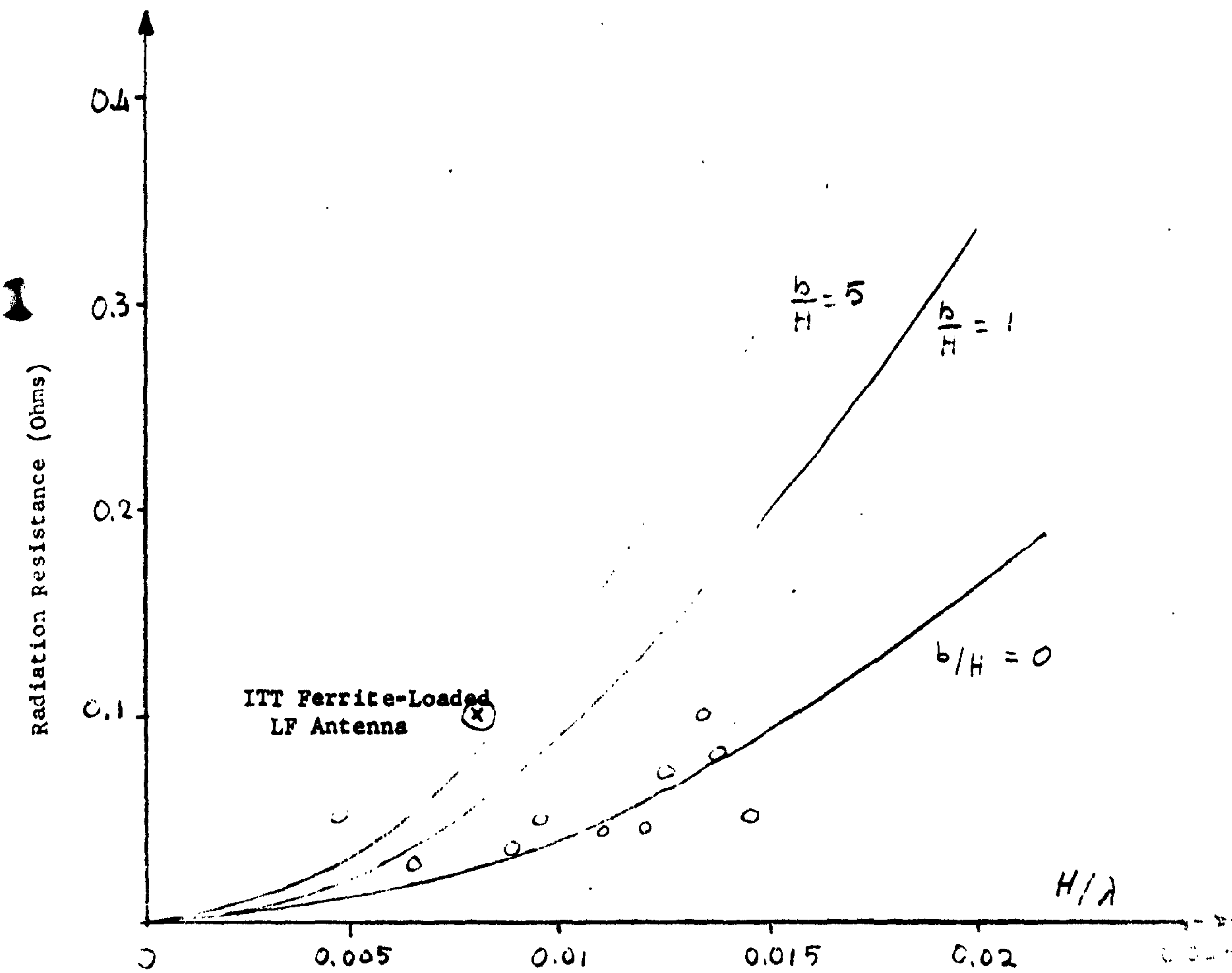

FIG. 14 - THEORETICAL AND EXPERIMENTAL VALUES OF RADIATION RESISTANCE VERSUS H/λ

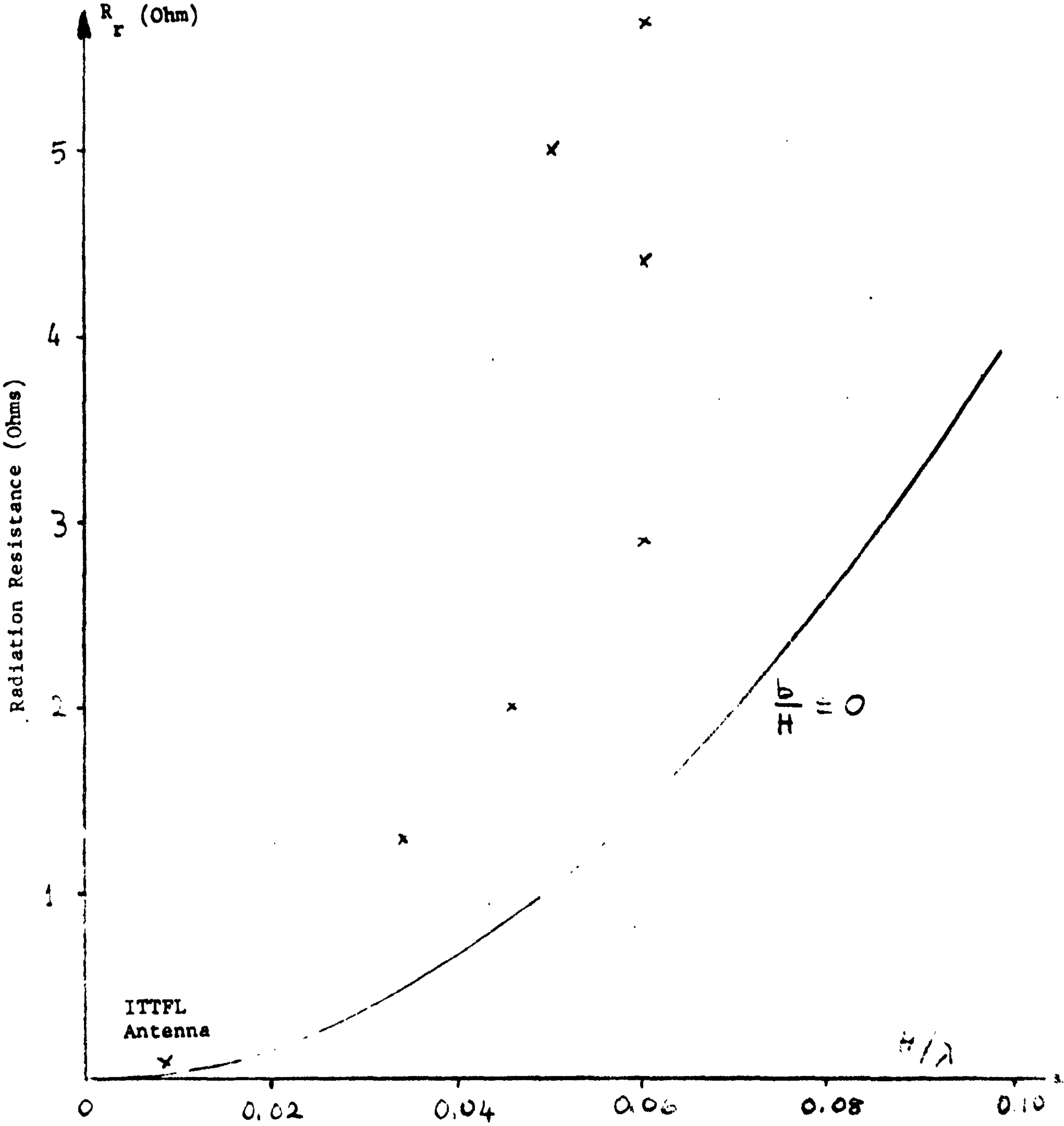

FIG. 15 - EXPERIMENTAL VALUES OF R_r FOR VARIOUS FERRITE-LOADED ANTENNAS VERSUS H/λ

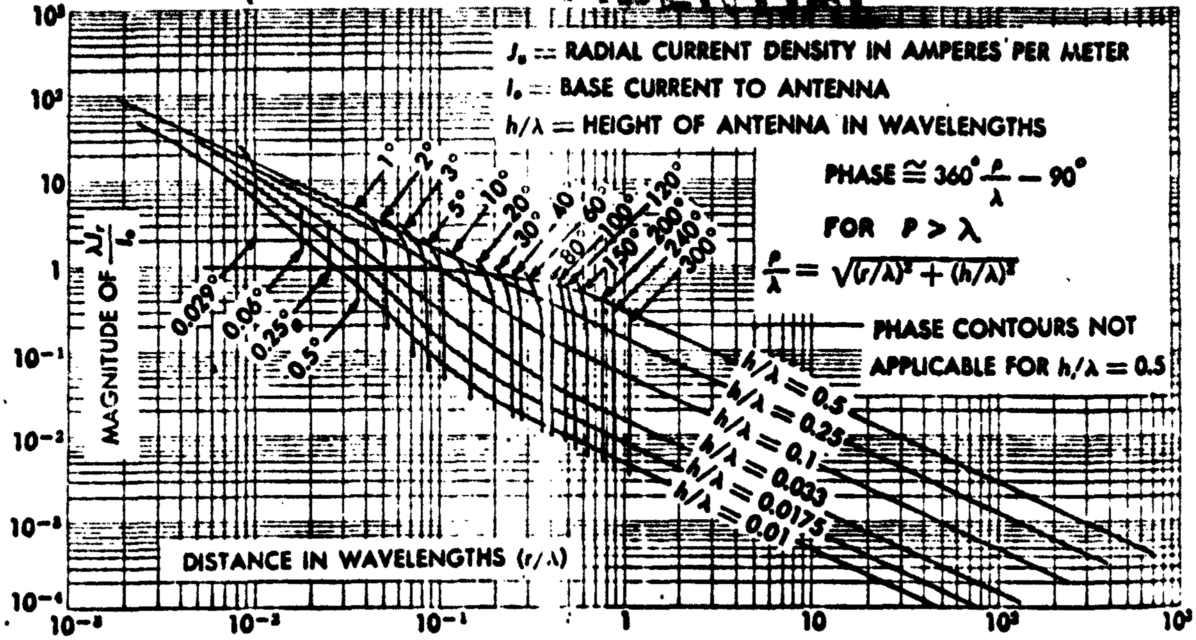

Fig. 16—Phase and density of radial ground current.

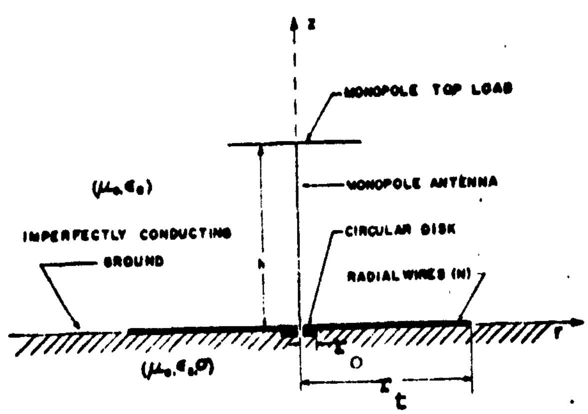

FIGURE 17- Sketch of antenna system.

CONFIDENTIAL

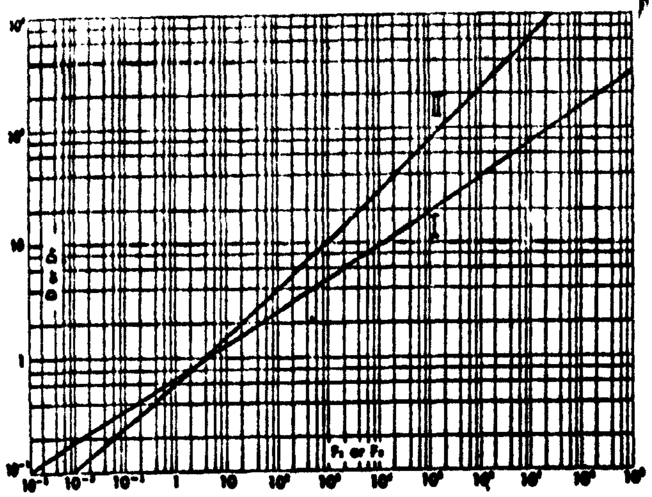

FIG. 18 - OPTIMUM AND TERMINAL SPACING OF BURIED CONDUCTORS.

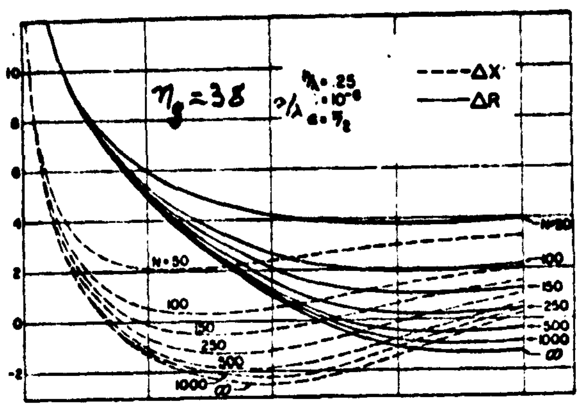

FIG. 19 - ΔR and ΔX vs r_t/λ ($h/\lambda = 0.25$).

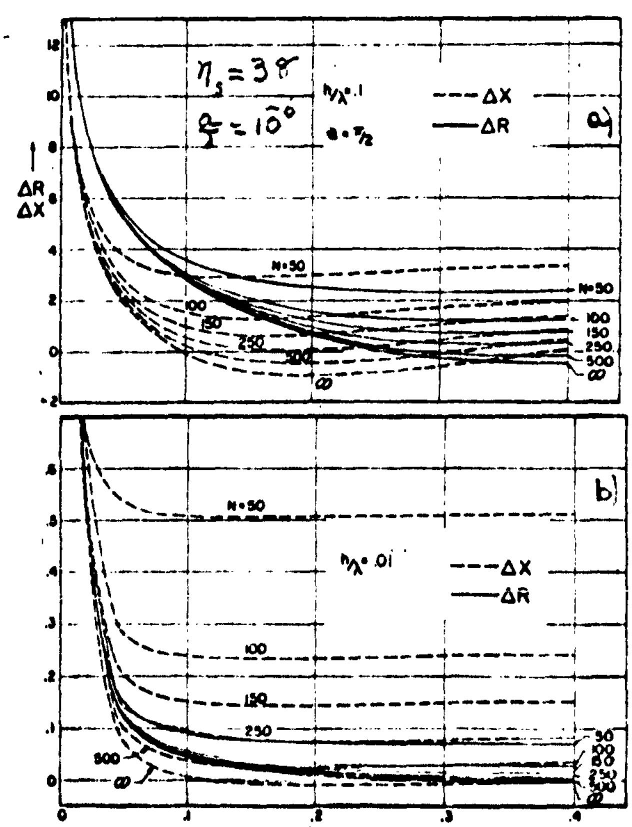

FIG. 20 - ΔR and ΔX vs r_t/λ ($h/\lambda = 0.1$ and 0.01)

CONFIDENTIAL

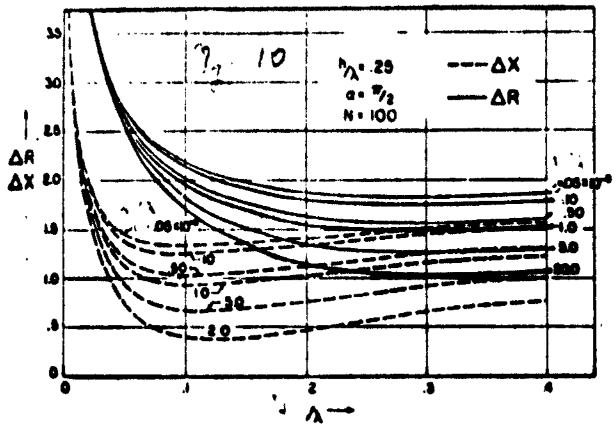

FIG. 21 - ΔR and ΔX VS r_t/λ
(PARAMETER a/λ)

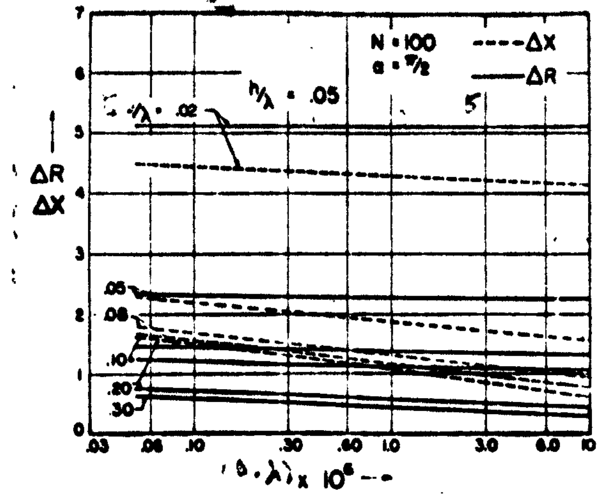

FIG. 22 - ΔR and ΔX VS a/λ
(PARAMETER r_t/λ)

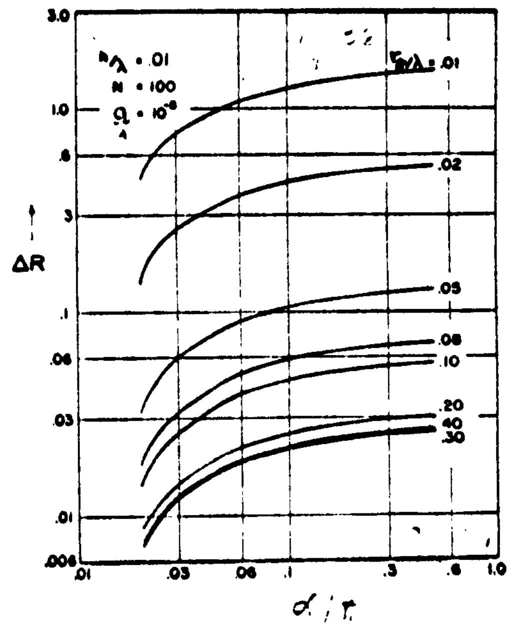

FIG. 23 - ΔR VS a/λ

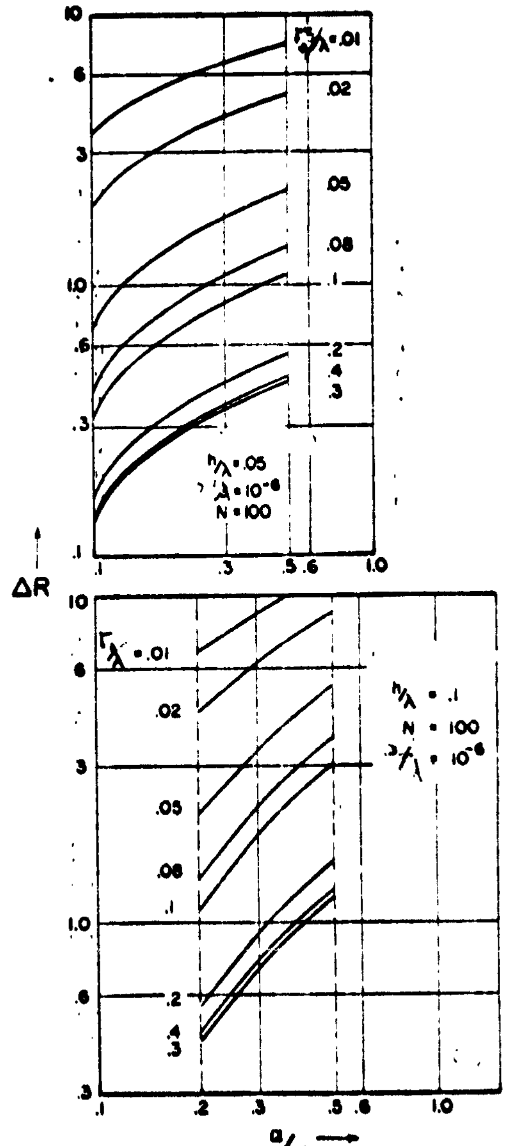

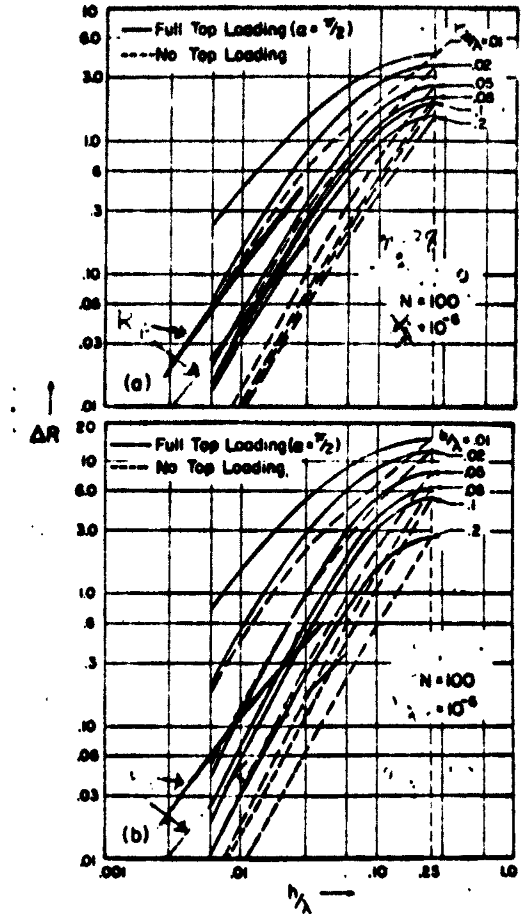

FIG. 24 - ΔR vs h/λ
(α = π/2 or 0)

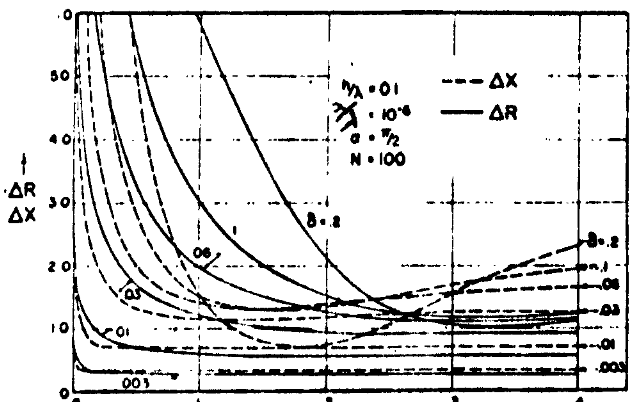

FIG. 25 - ΔR and ΔX vs r_t/λ FOR VARIOUS SURFACE IMPEDANCE VALUES.

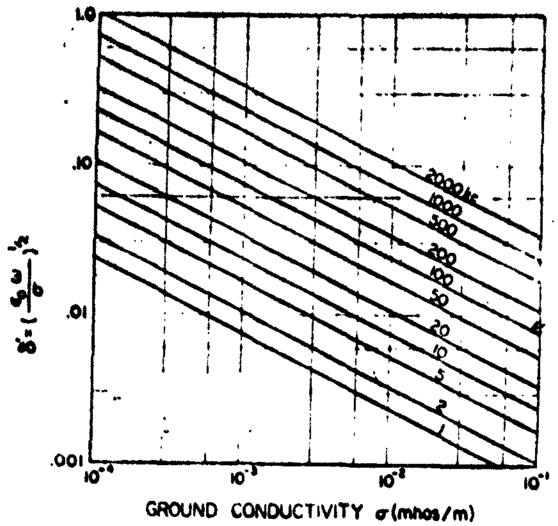

FIG. 26 - RELATIONSHIP BETWEEN AND GROUND CONDUCTIVITY.

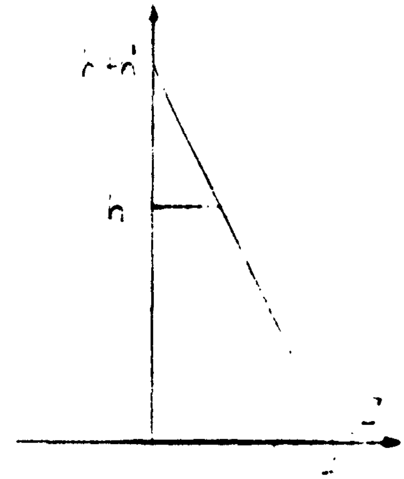

FIG. 27 - ASSUMED ANTENNA CURRENT DISTRIBUTION.

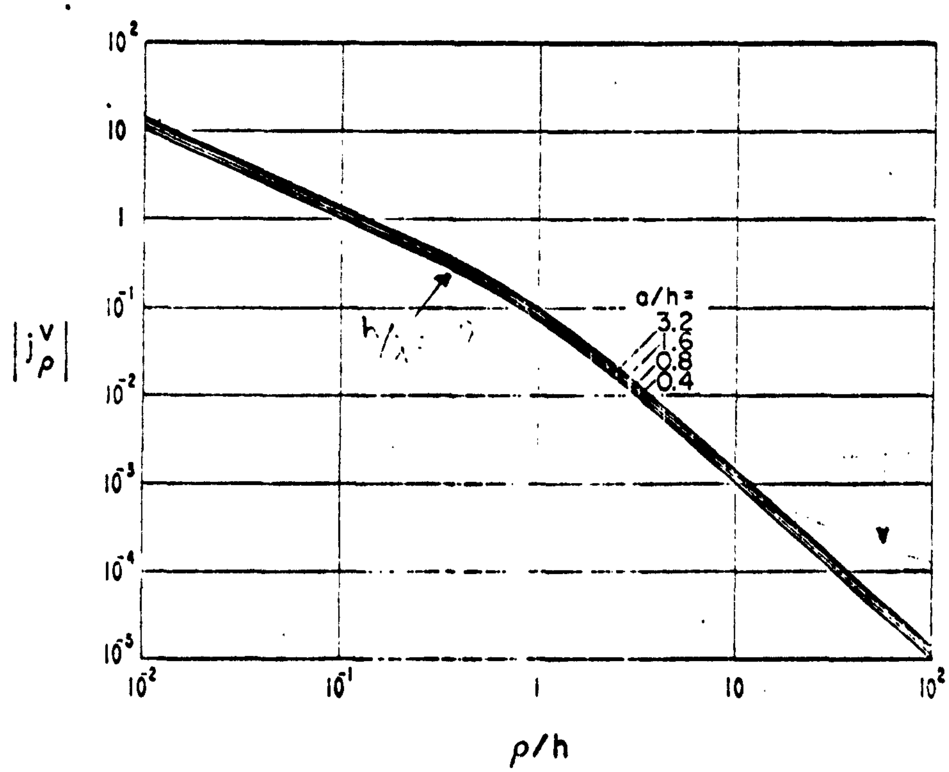

FIG. 28 - RADIAL DENSITY COMPONENT J_ρ^v vs ρ/h

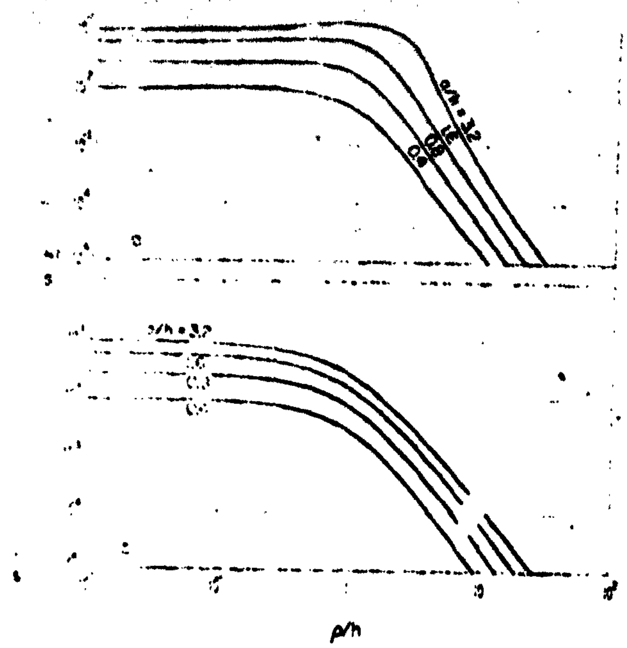

FIG. 29 - SURFACE CURRENT DENSITY J_s^h vs ρ/h AT TWO AZIMUTHS ($h/\lambda = 0$).

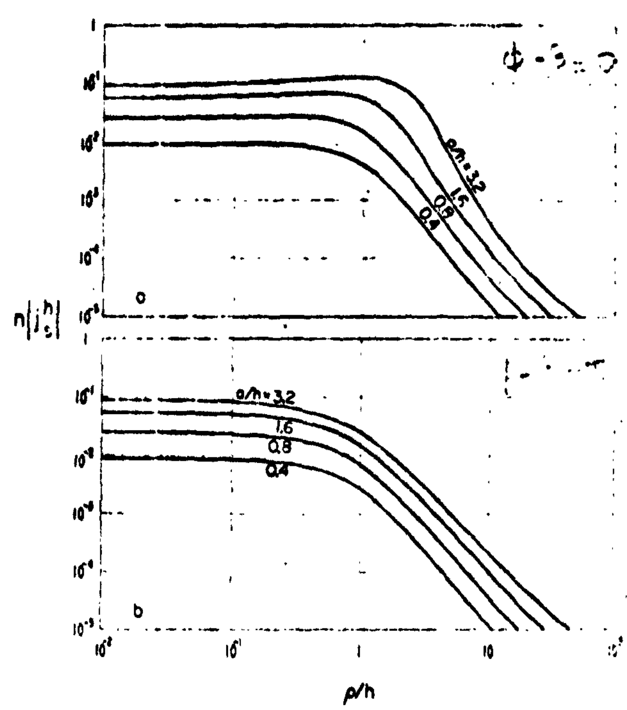

FIG. 30 - SURFACE CURRENT DENSITY J_s^h vs ρ/h AT TWO AZIMUTHS ($h/\lambda = 0.06$)

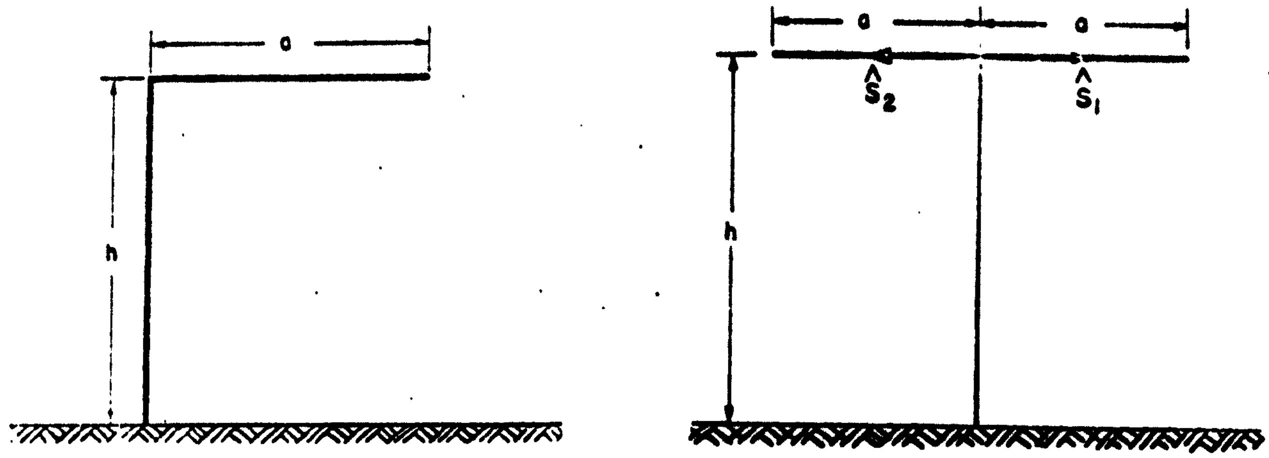

FIG. 31 - L- AND T-TYPE LOADING

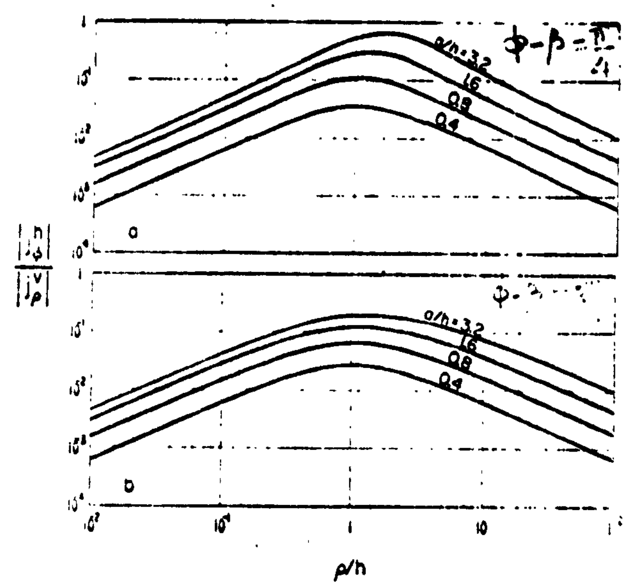

FIG. 32 - RATIO J_{ϕ}^{h} / J_{ρ}^{v} FOR
L-TYPE LOADING

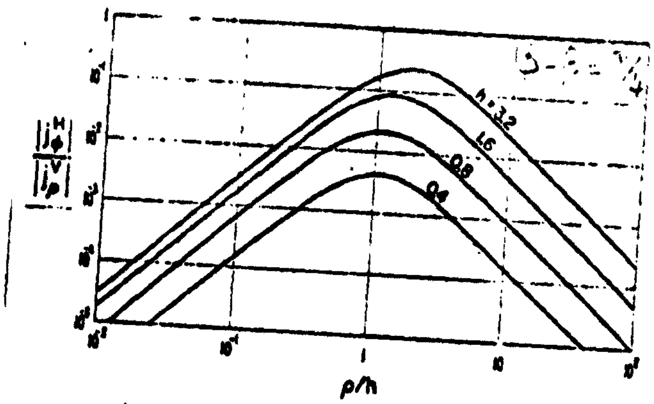

FIG. 33 - RATIO $J_\phi{}^h/J_\rho{}^v$ FOR T-TYPE LOADING ($h/\lambda = 0$)

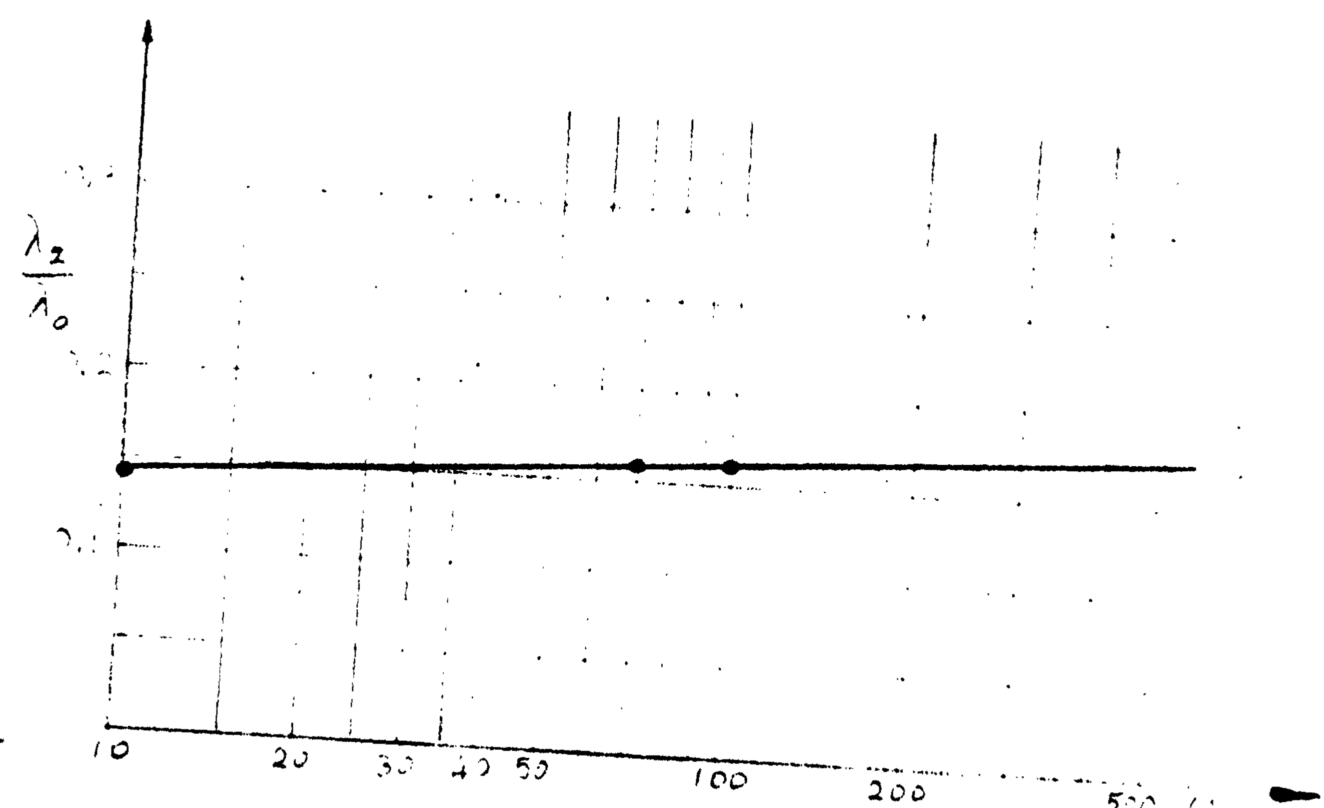

FIG. 34 - WAVELENGTH SHORTENING RATIO OF 3" FERRITE RADIATOR VS LENGTH.

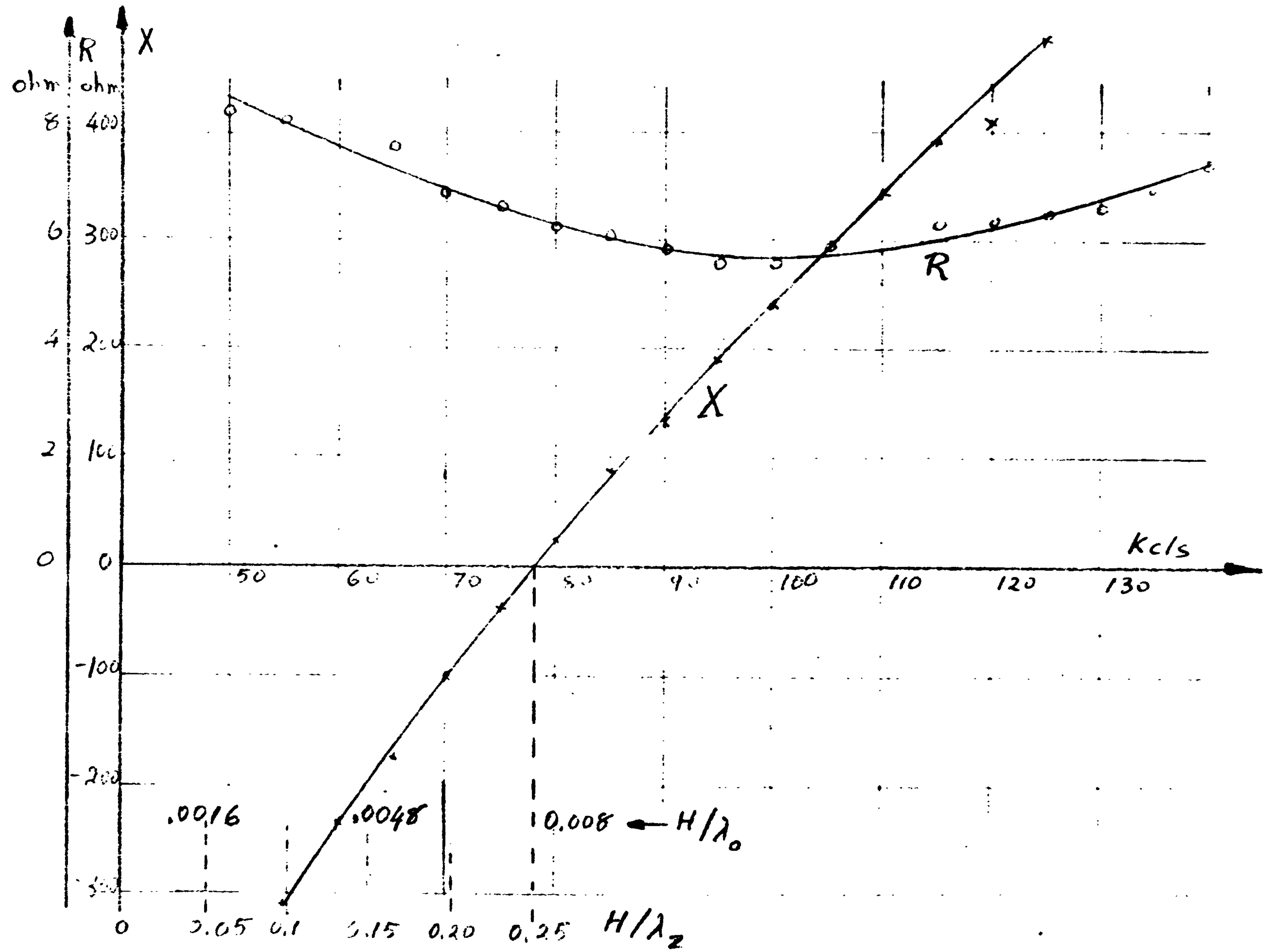

FIG. 35 - INPUT RESISTANCE AND REACTANCE OF 100-FT FERRITE RADIATOR

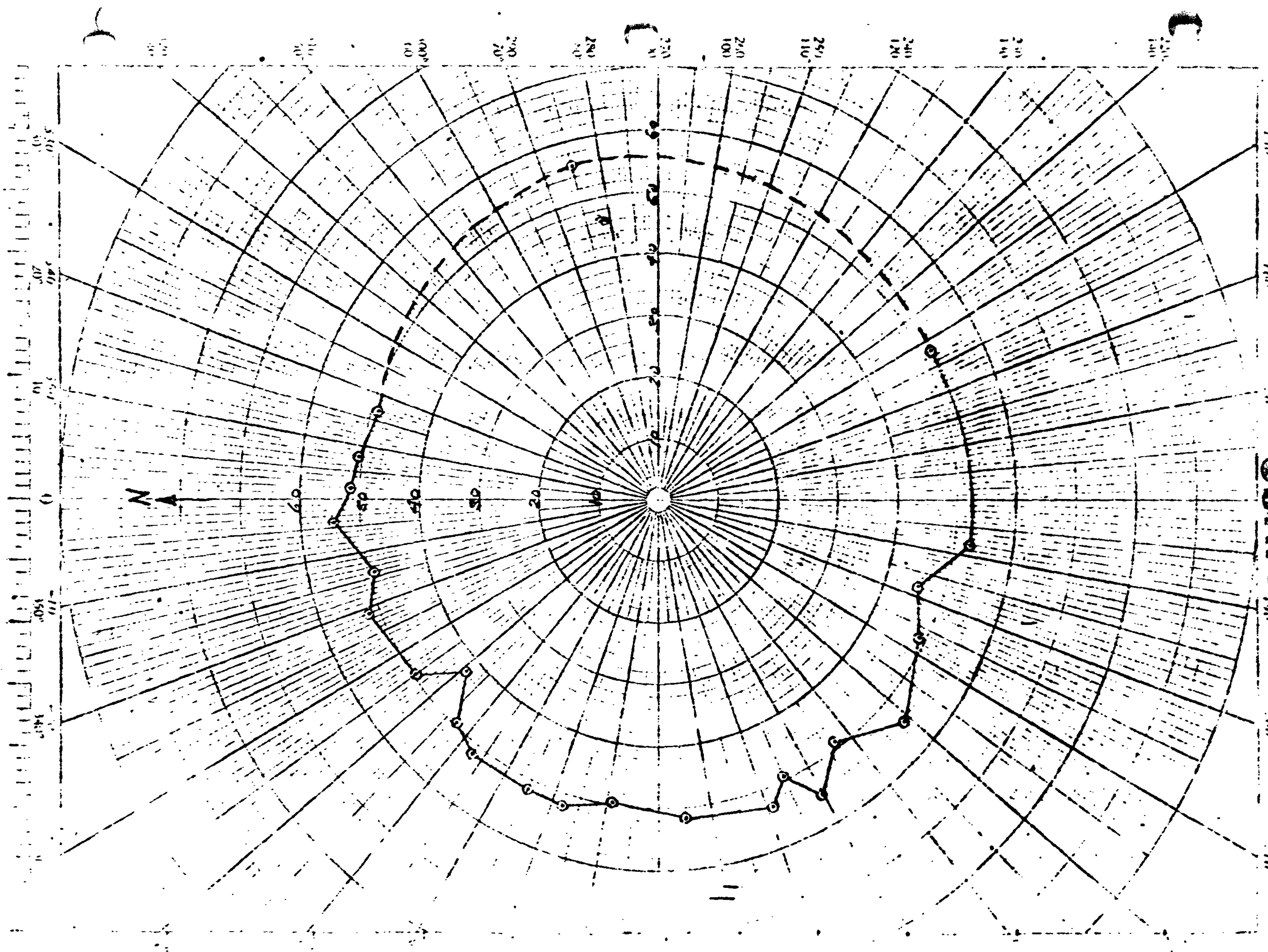

FIG. 36 - RADIATION PATTERN OF 100' FERRITE ANTENNA

DISTRIBUTION LIST

Addressee	No. of Copies
Defense Documentation Center Cameron Station, Building 5 5010 Duke Street Alexandria, Virginia 22314	20
Chief of Naval Research Electronics Branch (Code 427) Department of the Navy Washington 25, D.C.	[illegible]
Commanding Officer Office of Naval Research Branch Office 207 West 24th Street New York, N. Y. 10011	[illegible]
Chief of Naval Research Undersea Programs (Code 466) Department of the Navy Washington 25, D.C.	[illegible]
Director, Naval Research Washington 25, D.C. (Codes 2000, 5200)	Code 2000 - [illegible] Code 5200 - [illegible]
Commanding Officer Office of Naval Research (Box 39) Navy No. 100 Fleet Post Office New York, N.Y.	1
Director U. S. Naval Observatory Washington 25, D.C.	[illegible]
Chief, Bureau of Ships Department of the Navy Washington 25, D.C.	Code [illegible] - 1 Code 36[illegible]A - [illegible]
Chief, Bureau of Weapons Department of the Navy Washington 25, D.C.	[illegible]
Chief of Naval Operations (Op-70) Navy Department Washington 25, D.C.	[illegible]
Librarian U. S. Navy Post Graduate School Monterey, California	1
Mr. J. McLean (Code [illegible]) Office of the Director Defense Communication Agency Washington 25, D.C.	[illegible]